HHS Public Access

Author manuscript

J Immunol. Author manuscript; available in PMC 2018 November 01.

Published in final edited form as:

J Immunol. 2017 November 01; 199(9): 3348–3359. doi:10.4049/jimmunol.1700643.

PD-1 blockade promotes epitope spreading in anticancer CD8+ T cell responses by preventing fratricidal death of subdominant clones to relieve immunodomination

Arash Memarnejadian[*], **Courtney E. Meilleur**[*], **Christopher R. Shaler**[*], **Khashayarsha Khazaie**[†], **Jack R. Bennink**[‡], **Todd D. Schell**[§], and **S.M. Mansour Haeryfar**[*,¶,‖,#]

[*]Department of Microbiology and Immunology, Western University, London, Ontario, Canada

[†]Department of Immunology, Mayo Clinic College of Medicine, Rochester, Minnesota, USA

[‡]Laboratory of Viral Diseases, National Institute of Allergy and Infectious Diseases, National Institutes of Health, Bethesda, Maryland, USA

[§]Department of Microbiology and Immunology, The Pennsylvania State University, Hershey, Pennsylvania, USA

[¶]Department of Medicine, Division of Clinical Immunology & Allergy, Western University, London, Ontario, Canada

[‖]Centre for Human Immunology, Western University, London, Ontario, Canada

[#]Lawson Health Research Institute, London, Ontario, Canada

Abstract

The interactions between programmed death-1 (PD-1) and its ligands hamper tumor-specific $CD8^+$ T cell (T_{CD8}) responses, and PD-1-based 'checkpoint inhibitors' have shown promise in certain cancers, thus revitalizing interest in immunotherapy. PD-1-targeted therapies reverse T_{CD8} exhaustion/anergy. However, whether they alter the epitope breadth of T_{CD8} responses remains unclear. This is an important question because subdominant T_{CD8} are more likely than immunodominant clones to escape tolerance mechanisms and may contribute to protective anticancer immunity. We have addressed this question in an *in vivo* model of T_{CD8} responses to well-defined epitopes of a clinically relevant oncoprotein, large T antigen. We found that unlike other co-inhibitory molecules (CTLA-4, LAG-3, TIM-3), PD-1 was highly expressed by subdominant T_{CD8}, which correlated with their propensity to favorably respond to PD-1/PD-L1-blocking antibodies. PD-1 blockade increased the size of subdominant T_{CD8} clones at the peak of their primary response, and also sustained their presence giving rise to an enlarged memory pool. The expanded population was fully functional as judged by IFN-γ production and MHC I-restricted cytotoxicity. The selective increase in subdominant T_{CD8} clonal size was due to their enhanced survival, not proliferation. Further mechanistic studies utilizing peptide-pulsed dendritic cells, recombinant vaccinia viruses encoding full-length T antigen or epitope mingenes, and tumor cells expressing T antigen variants revealed that anti-PD-1 invigorates subdominant T_{CD8}

Corresponding author: Dr. S.M. Mansour Haeryfar. Telephone: (519) 850-2488; Fax: (519) 661-3499; Mansour.Haeryfar@schulich.uwo.ca.

responses by relieving their lysis-dependent suppression by immunodominant T_{CD8}. Our work constitutes the first report that interfering with PD-1 signaling potentiates epitope spreading in tumor-specific responses, a finding with clear implications for cancer immunotherapy and vaccination.

Introduction

$CD8^+$ T cells (T_{CD8}) play a pivotal role in immune surveillance against spontaneously arising neoplastic cells and in controlling intracellular pathogens. However, when the immune system fails to eradicate cancer or clear stubborn infections, prolonged antigenic stimulation may lead to T_{CD8} functional impairments, including exhaustion and anergy (1–4). Exhausted or anergic T_{CD8} are often unable to secrete effector cytokines or launch optimal proliferative and cytotoxic responses to cognate Ags, which may compromise host defense mechanisms, positive clinical outcomes or even survival (5–7).

Of several co-inhibitory molecules known to interfere with *bona fide* T_{CD8} activation, programmed death-1 (PD-1, CD279) has emerged as a major mediator of exhaustion and anergy (8). PD-1 is a type I transmembrane protein expressed by cells of hematopoietic origin including T cells (9, 10). TCR triggering drives the expression of PD-1 at both transcriptional and translational levels (11, 12), which subsides once the Ag source is removed. However, PD-1 remains upregulated if TCR engagement is sustained, for instance in individuals with high tumor burden. Once ligated, PD-1 is phosphorylated on its intracellular tyrosine residues, which in turn leads to enhanced recruitment of Src homology 2 (SH2)-containing tyrosine phosphatase-1 (SHP-1) and SHP-2 to PD-1's immunoreceptor tyrosine-based switch motif (13), thus dampening signal transduction through phosphoinositide 3-kinase and the TCR complex (10).

PD-1 binds to two distinct ligands, namely PD-L1 (*aka*. B7-H1 or CD274) (14, 15) and PD-L2 (*aka*. B7-DC or CD273) (16, 17). PD-L1 is expressed, constitutively or inducibly, by a variety of hematopoietic and non-hematopoietic cells (10), and in various types of cancer (18). By contrast, PD-L2 has a much more restricted expression pattern and is primarily found on activated macrophages and myeloid dendritic cells (DCs) (10).

'Checkpoint inhibitors' that block PD-1-PD-L1 interactions have shown promise in preclinical studies and in clinical trials for several types of cancer (19, 20). Unfortunately however, not all malignancies respond favorably to PD-1-targeted therapies. This highlights the need to better understand how the PD-1-PD-L1 pathway operates to incapacitate antitumor responses (21, 22).

Blocking the PD-1-PD-L1 axis improves T_{CD8} responses by relieving co-inhibition during T_{CD8} priming by APCs, by preventing the lysis of effector T_{CD8} by $PD\text{-}L1^+$ tumors or virus-infected cells, and by reinvigorating exhausted T_{CD8} (23). While these effects clearly benefit host defense mechanisms, many, if not most, studies to date have focused on the effects of PD-1 signaling or blockade on T_{CD8} that recognize immunodominant determinants (IDDs) of tumor and viral Ags. While logistically convenient and still valid, this approach may overlook a critical aspect of T_{CD8} responses – that is their epitope breadth. This is

concerning in light of the growing appreciation that immunodominant T_{CD8} may not necessarily be the most protective clones (24). Importantly, whether signaling through PD-1, or its blockade, broadens or narrows T_{CD8} responses is essentially unexplored.

Complex Ags harbor thousands of potentially immunogenic peptides; yet, only a 'selected' few induce detectable T_{CD8} responses of varying magnitude, which are reproducibly arranged in a hierarchical order. This intriguing phenomenon is called immunodominance (ID) (25). We and others have demonstrated that T_{CD8} ID can be shaped by Ag dose and administration route (26, 27), T_{CD8} priming pathway (*i.e.*, direct priming *versus* cross-priming) (28) and the type of APCs involved (29), abundance of protein substrates (30), efficiency and kinetics of peptide liberation by standard proteasomes and immunoproteasomes (31, 32), degenerate selectivity of TAP for peptides (33), peptide binding affinity for MHC class I allomorphs (33, 34), presence and precursor frequency of cognate T_{CD8} in one's T cell repertoire (35), TCR structural diversity, for instance due to N-nucleotide addition within junctional sequences (36, 37), selective suppression of T_{CD8} responses by naturally occurring regulatory T (nTreg) cells (38), and immunomodulatory actions of certain intracellular enzymes such as IDO (39) and mammalian target of rapamycin (mTOR) (40). Additionally, immunodominant T_{CD8} clones may outcompete subdominant clones for access to APCs (41) or even directly kill them although the evidence for the latter scenario has been scarce.

It is important to note that the above factors and mechanisms contribute to but do not fully account for ID. In this work, we demonstrate for the first time to our knowledge that: **i)** PD-1, unlike several other receptors implicated in T cell co-inhibition or exhaustion, enforces ID disparities in T_{CD8} responses to a clinically relevant oncoprotein; **ii)** blockade of PD-1-PD-L1 interactions increases the epitope breadth of tumor-specific T_{CD8} responses, thus increasing the range of peptide epitopes that can be targeted by the host; **iii)** treatment with anti-PD-1 prevents immunodomination otherwise exerted by immunodominant T_{CD8} through a fratricidal mechanism. These findings shed new light on T_{CD8} ID and also have clear implications for immunotherapy of cancer and potentially other conditions such as chronic viral diseases.

Materials and Methods

Mice

Female C57BL/6 (B6) mice were purchased from Charles River Canada Inc. (St. Constant, Quebec) and housed in our institutional barrier facility. Closely age-matched, adult mice were used following an animal use protocol approved by the Western University Animal Use Subcommittee and the Canadian Council on Animal Care guidelines.

Cell lines

The mouse mastocytoma cell line P815 was grown in RPMI 1640 medium containing 10% heat-inactivated FBS, GlutaMAX-I, 0.1 mM MEM nonessential amino acids, 1 mM sodium pyruvate and 50 μM 2-ME.

We and/or others have previously described the generation of several cell lines that enable *in vivo* monitoring of SV40 large tumor antigen (T Ag)-specific T_{CD8} responses. C57SV cells are transformed fibroblasts on the B6 (H-2^b) background (42, 43), and KD2SV cells (H-2^d) are of kidney epithelial origin (40, 43, 44). The TAP1$^{-/-}$ wt T Ag line was generated by transfecting primary mouse kidney cells from B6.129S2-Tap1^{tm1Arp} mice with pPVU0, a plasmid containing the intact SV40 early region (45). B6/K-TagI cells were derived from B6 primary kidney cells transformed with pLM506-G(DC-1), a plasmid that was designed to encode a T Ag mutant with alanine substitutions at positions N227, F408 and N493. These amino acids comprise critical MHC I anchor residues within T Ag's sites II/III, IV and V epitopes, respectively (46). B6/TpLM237-9Ab cells are B6 mouse embryonic fibroblasts transformed through expression of a site IV-loss variant of T Ag containing a deletion of residues 404–411 (47). All T Ag$^+$ cell lines were maintained in DMEM supplemented with 10% FBS.

Peptides

Peptides used in this investigation are listed in Table 1. They were procured or synthesized, purified by HPLC, and analyzed by mass spectrometry at or under the supervision of the Research Technologies Branch, NIAID (Rockville, MD), to confirm a purity of >95%. Stock solutions were prepared at 1 mM in DMSO and stored at −30°C.

Inoculation with tumor cells or recombinant vaccinia viruses (rVVs)

Monolayers of tumor cell lines were trypsinized after they reached 100% confluency. Cells were washed thoroughly and resuspended in sterile PBS. To prime B6 mice, 2×10^7 cells tumor cells were injected i.p.

rVV-FL T Ag, which expresses full-length T Ag, and rVV-I minigene that encodes T Ag's site I epitope as a cytosolic minigene were initially provided by Dr. Satvir Tevethia (Pennsylvania State University, Hershey, PA), and propagated in the thymidine kinase-deficient human osteosarcoma cell line 143B. To infect mice, 1×10^6 PFUs of each rVV were injected i.p.

Immunization with peptide-pulsed DCs

Bone marrow-derived DCs (BMDCs) were generated by culturing marrow cells with recombinant mouse GM-CSF and IL-4 as previously described (39), and matured using 100 ng/mL LPS during the final 16 h of the culture. Adherent and floating DCs were harvested and pulsed for 2 h at 37°C with synthetic peptides corresponding to T Ag's site I and/or site IV (Table 1) at a final concentration of 1 μM. Cells were then washed thrice and resuspended in sterile PBS before $5–10 \times 10^5$ BMDCs were injected into the tail vein of each mouse.

Treatment protocols

Two h before inoculation with tumor cells, rVVs or peptide-pulsed DCs, mice received 100 μg of an anti-mouse PD-1 mAb (clone RMP1-14) or a rat IgG2a isotype control (clone 2A3) i.p. Animals received two additional 100-μg doses of anti-PD-1 or isotype on days 3 and 6. Following an identical protocol, we treated separate cohorts of mice, where indicated, with an anti-PD-L1 mAb (clone 10F.9G2) or rat IgG2b (clone LTF-2), or with a combination of

anti-PD-1 and anti-PD-L1 mAbs (or isotype controls). To inactivate nTreg cells, a 1-mg single i.p. injection of an anti-mouse CD25 mAb (clone PC-61.5.3) was given 3 days prior to priming with C57SV cells. Control animals received a rat IgG1 (clone HRPN). The above mAbs and isotype controls were all purchased from BioXCell (West Lebanon, NH).

Tetramer and intracellular cytokine staining

Unless otherwise specified, mice were euthanized 9 days after priming with T Ag^+ tumor cells or 7 days after infection with rVVs or immunization with peptide-pulsed BMDCs. These time points coincide with the peak of *in vivo* T_{CD8} responses to T Ag- and rVV-derived epitopes (38, 48), and T_{CD8} responses after DC vaccination are often detectable after 7 days.

Splenic cell preparations were depleted of erythrocytes before they were washed, filtered and stained. In a limited number of experiments, peripheral blood was collected into heparinized micro-hematocrit capillary tubes, diluted 1:2 in sterile PBS, and overlaid on 500 μL of low-endotoxin (<0.12 EU/mL) Ficoll-Paque PLUS. Cells were spun at 400 × *g* for 30 min at room temperature, and PBMCs gathering at the plasma-Ficoll interface were gently harvested and washed. Peritoneal exudate cells (PECs) were collected via peritoneal lavage in several experiments in which mice had received i.p. injections of tumor cells.

We have previously described MHC class I tetramer reagents that enable sensitive quantitation of T Ag-specific T_{CD8} responses (48). Splenocytes from naïve and primed B6 mice were placed at a density of 2×10^6 cells/well in a round-bottom microplate and exposed to 20 μL of the 2.4G2 hybridoma supernatant containing an anti-CD16/CD32 mAb on ice to prevent non-specific, FcγR-mediated adherence of Abs. After 20 min, cells were washed and resuspended in 2% FBS containing a PE-conjugated anti-mouse CD8α mAb (clone 53–6.7) and allophycocyanin-conjugated H-$2K^b$/IV or H-$2D^b$/I tetramer, which were used at a 1:200 dilution. Cells were incubated for 15 min in dark at room temperature, washed twice and immediately interrogated by flow cytometry. Naïve B6 splenocytes served as a negative staining control to allow for proper gating. In several experiments, surface staining for CTLA-4, LAG-3, PD-1, TIM-3 and CD107a and intracellular staining for Ki-67 were conducted in conjunction with tetramer staining. To detect CD107a, splenocytes were simultaneously exposed to antigenic peptides and stained with an Alexa Fluor® 647-conjugated rat anti-mouse CD107a mAb (clone 1D4B) in the presence of 1 μM monensin before they were subjected to tetramer staining. A BD FACSCanto II cytometer and FlowJo software (Tree Star, Ashland, OR) were employed for data acquisition and analysis, respectively.

Intracellular cytokine staining (ICS) for IFN-γ was performed using a standard protocol. Erythrocyte-depleted splenocytes, PECs or PBMCs were suspended in medium and seeded at $0.5–2 \times 10^6$ cells/well of a round-bottom microplate. Cells were left untreated or stimulated with indicated T Ag^+ tumor cells or synthetic peptides corresponding to T Ag-derived T_{CD8} epitopes (Table 1). Peptides were used at a final concentration of 500 nM. After 2-h incubation at 37°C, 10 μg/mL of brefeldin A was added to each well to retain IFN-γ in the endoplasmic reticulum of activated T_{CD8}, and cultures were continued for an additional 3–4 h. Cells were subsequently washed, briefly incubated with anti-CD16/CD32,

and stained for surface CD8α before they were washed, fixed with 1% paraformaldehyde, washed again, permeabilized with 0.1% saponin and stained for intracellular IFN-γ. The frequency of IFN-γ^+ cells was determined after live gating on CD8α^+ events, which was used to also calculate Ag-specific T_{CD8} numbers in each spleen.

All fluorochrome-labeled mAbs were from eBioscience or BD Biosciences except for anti-CD107a that was purchased from BioLegend.

In vivo cytotoxicity assay

We have previously described a modified, 'three-peak' version of *in vivo* cytotoxicity assays to study T_{CD8} ID (37). Syngeneic splenocytes were split into three populations, each of which was pulsed for 1 h at 37°C with 1 μM of an irrelevant or cognate peptide and labeled with a given dose of CFSE as follows. Control target cells were coated with an H-2^b-binding immunodominant peptide of HSV-1, namely gB_{498}, and 0.025 μM CFSE ($CFSE^{low}$). Splenocytes that were pulsed with site II/III or site I and stained with 0.25 μM ($CFSE^{int}$) or 2 μM CFSE ($CFSE^{high}$), respectively, served as cognate target cells. Cells were washed and mixed in equal numbers before a total of 2×10^7 cells in PBS were injected i.v. into naïve and primed B6 mice. Four h later, mice were sacrificed for their spleens, which were immediately homogenized and transferred onto ice. Up to 2×10^3 $CFSE^{low}$ events were acquired for each spleen, and the specific lysis of target cells was calculated using the following formula: % specific killing = {1 – [$CFSE^{int/high}$ event number in T Ag-primed mouse ÷ $CFSE^{low}$ event number in T Ag-primed mouse) ÷ ($CFSE^{int/high}$ event number in naive mouse ÷ $CFSE^{low}$ event number in naive mouse)]} × 100.

Measurement of cognate T_{CD8} apoptosis

A CaspaTag™ Pan-Caspase In Situ Assay Kit from Chemicon® (Catalogue # APT420) was used to identify T_{CD8} undergoing apoptosis based on the ability of fluorochrome-labeled inhibitors of caspases (FLICA) to enter cells and covalently bind to, label and irreversibly inhibit active caspases (49). The FLICA probe utilized in this kit was the green fluorescent, cell-permeable, nontoxic pan-caspase inhibitor FAM-VAD-FMK. Splenocytes from anti-PD-1- and isotype-treated animals were stained with an allophycocyanin-conjugated anti-CD8α mAb and PE-conjugated H-$2K^b$/IV or H-$2D^b$/I tetramer before they were exposed to the FLICA reagent as per manufacturer's instructions. The frequency of sites I- and IV-specific T_{CD8} emitting a green signal was determined by flow cytometry.

T cell proliferation in response to non-specific mitogens

Splenocytes from anti-PD-1- and isotype-treated mice were seeded at 5×10^5 cells/well of a round-bottom microplate. Cells were stimulated with a 1:20 dilution of the 145-2C11 hybridoma supernatant containing ~0.25 μg/mL of an anti-CD3ε mAb, with 5 μg/mL of Con A, or with a combination of 50 ng/mL of PMA and 500 ng/mL of ionomycin. Plates were kept at 37°C and 6% CO_2 for 72 h, and cells were exposed to 1 μCi of tritiated thymidine ([^{3}H]TdR) during the final 18 h of the incubation period. Cultures were harvested onto glass fiber filter mats and [^{3}H]TdR incorporation into replicating DNA was quantified by liquid scintillation counting.

Statistical analyses

Statistical comparisons were carried out with the aid of GraphPad Prism 6 software. We used parametric Student's *t*-tests or ANOVA with Holm-Sidak post-hoc analysis as appropriate. *, **, *** and **** denote differences with $p<0.05$, $p<0.01$, $p<0.001$ and $p<0.0001$, respectively.

Results

PD-1 is highly and preferentially expressed on subdominant antitumor T_{CD8}

Despite intense investigations on ID, whether a subdominant status within T_{CD8} hierarchies can be due to exhaustion/anergy or at least correlated with co-inhibitory proteins T_{CD8} may express is unclear. To begin to address this neglected but important question, we examined the expression of classic co-inhibitory molecules, namely CTLA-4, PD-1, LAG-3 and TIM-3, by T_{CD8} in an *in vivo* model of ID in which the SV40-encoded T Ag is targeted.

Priming B6 mice with SV40-transformed, T Ag^+ tumor cells generates T_{CD8} clones that recognize four well-defined peptide epitopes of T Ag, termed sites I, II/III, IV, and V (Table 1) (38, 43, 48). Site IV is an IDD by virtue of its ability to elicit a rigorous proliferative response, whereas sites I and II/III are considered subdominant determinants (SDDs), and site V-specific T_{CD8} are 'immunorecessive' and only measurable when recognition of the other epitopes is absent (48, 50). Therefore, T Ag-specific T_{CD8} display the following rank order: site IV >> I ≥ II/III >> V.

Nine days after inoculation of B6 mice with C57SV cells, a syngeneic T Ag^+ cancer cell line, T_{CD8} specific for sites IV and I, respectively representing IDDs and SDDs, were readily detectable by tetramer staining in the spleens (Fig. 1A). Cytofluorimetric analysis of sites I- and IV-specific T_{CD8} revealed no expression of CTLA-4, LAG-3 or TIM-3 (Fig. 1A–B). However, over 80% of both T_{CD8} populations stained positively for PD-1 (Fig. 1B). Interestingly however, PD-1 expression on a per cell basis, as judged by the mean fluorescence intensity (MFI) of PD-1, was significantly and reproducibly higher among subdominant site I-specific T_{CD8} present in the spleen (Fig. 1C) and within the peritoneal cavity (with an average geometric MFI of 904 and 630 for sites I- and IV-specific peritoneal T_{CD8}, respectively). Given the i.p. route of C57SV cell injection, peritoneal and splenic T_{CD8} responses provide a picture of local and systemic reactivity to T Ag, respectively.

In vivo treatment with anti-PD-1 selectively enlarges the subdominant site I-specific T_{CD8} population size

To explore whether the high expression level of PD-1 by site I-specific T_{CD8} is biologically significant and could potentially mean higher susceptibility to PD-1 blockade, we administered three separate doses of a blocking anti-PD-1 mAb or isotype control to mice that were injected with C57SV cells. We found that unlike site IV-specific T_{CD8} whose percentage increased only marginally in anti-PD-1-treated animals, site I-specific T_{CD8} population almost tripled in size (Fig. 2A). This was not a global effect because T cell proliferation in response to non-specific stimuli that work by cross-linking TCRs (*e.g.*, anti-

CD3ε and Con A) or bypass TCR ligation (PMA plus ionomycin) was comparable in anti-PD-1- and isotype-treated mice (Fig. 2B).

PD-1-PD-L1 axis blockade increases the frequency of IFN-γ$^+$ SDD-specific T_{CD8} in the T Ag immunization model

Tetramer reagents identify T_{CD8} bearing TCRs of unique specificity for a given peptide:MHC I complex without providing any information on their functional competence. It was thus pertinent to ascertain whether T Ag-specific T_{CD8} whose frequency rose upon anti-PD-1 treatment retained their effector functions including their ability to secrete cytokines. To this end, we performed ICS for IFN-γ, the prototypic effector cytokine of T_{CD8}, to enumerate functional T cells recognizing each of the four peptide epitopes of T Ag. Blocking PD-1 dramatically increased both the frequency and the absolute number of site I-specific, IFN-γ-producing T_{CD8} in the spleen (Fig. 3A). A similar enhancement was observed, albeit to a slightly lesser degree, for T_{CD8} targeting site II/III, the other SDD in the T Ag model, (Fig. 3A). Consistent with tetramer staining findings (Fig. 2A), anti-PD-1 failed to elevate the percentage of site IV-specific, IFN-γ$^+$ T_{CD8}. Interestingly, the MFI of IFN-γ remained unaltered across all four T_{CD8} clones. To be exact, the mean MFI ± SEM of IFN-γ in isotype- and anti-PD-1-treated mice (n=19 per group) was 1,434 ± 171 *vs.* 1,453 ± 171 (site I), 1,382 ± 206 *vs.* 1,268 ± 125 (site II/III), 1,711 ± 152 *vs.* 1,504 ± 123 (site IV) and 1,220 ± 130 *vs.* 1,031 ± 99 (site V), respectively. Therefore, PD-1 blockade raises the frequencies of T Ag-derived SDD-specific T_{CD8} without changing their IFN-γ production capacity.

Our kinetic studies yielded two additional observations. First, the boosting effect of anti-PD-1 on site I manifested itself at a relatively late time point such that the curves corresponding to anti-PD-1 and isotype control segregated only after day 6 (Fig. 3B). This suggests that PD-1 blockade does not affect the early phase of naïve T_{CD8} activation. Second, in anti-PD-1-treated animals, the response against site I continued to rise after day 9, the expected peak of T Ag-specific T_{CD8} responses (48), and was even more vigorous on day 12 (Fig. 3B). We also assessed memory T_{CD8} responses to T Ag epitopes 3 weeks after C57SV cell inoculation, and demonstrated that the enhancing effect of anti-PD-1 on sites I- and II/III-specific, but not site IV-specific, T_{CD8} was still evident (Supplemental Fig. 1).

Next, we compared the efficacy of anti-PD-1 and anti-PD-L1. Anti-PD-L1 was found to mimic the enhancing impact of anti-PD-1 on sites I- and II/III-specific T_{CD8} (Fig. 3C). Furthermore, combining the two mAbs did not increase the frequency of subdominant T_{CD8} beyond the levels achieved by either anti-PD-1 or anti-PD-L1 alone (Fig. 3C). These results, indicate that: **i)** PD-1-PD-L-1 interactions curb T_{CD8} responses to SDDs; **ii)** PD-1- and PD-L1-blocking mAbs should be equally effective in augmenting subdominant T_{CD8} responses in similar experimental or therapeutic settings.

Finally, the preferential effect of anti-PD-1 on subdominant T_{CD8} was not limited to the spleen, and could also be observed in the peripheral blood (Fig. 3D). Collectively, the above results indicate that interfering with PD-1-PD-L-1 interactions results in a numerical increase in subdominant tumor Ag-specific T_{CD8} that maintain their IFN-γ production capacity.

T_{CD8}-mediated cytotoxicity against T Ag's SDDs is augmented following anti-PD-1 administration

The ultimate role of T_{CD8} in cancer immunity is to kill malignant cells displaying cognate peptide:MHC I complexes. Therefore, we employed an *in vivo* killing assay to extend our findings to this important function. CFSE-labeled syngeneic splenocytes were coated with synthetic peptides corresponding to T Ag epitopes or an IDD of HSV-1, gB_{498}, which was used as an irrelevant peptide. Control and cognate target splenocytes were mixed, injected i.v. into naïve or C57SV-primed B6 mice, and tracked after 4 h. While target cells remain intact in naïve mice, site IV-coated cells are quickly and completely destroyed in primed animals regardless of the treatment they receive. As expected, gB_{498}-coated target cells were not removed from the spleens (Fig. 4A). Importantly, in comparison with the control cohort, anti-PD-1-treated mice exhibited substantially higher cytolytic activities against sites I- and II/III-pulsed splenocytes (Fig. 4A–B). In separate experiments, we found that almost all IFN-γ^+ T_{CD8} and the majority of tetramer$^+$ T_{CD8} expressed the degranulation marker CD107a (data not shown). Furthermore, CD107a$^+$ cell frequencies and CD107a expression levels were comparable in control and anti-PD-1-treated mice (data not shown). These findings demonstrate that PD-1 blockade gives rise to an enlarged pool of cytotoxic T lymphocytes capable of targeting the SDDs of T Ag.

PD-1 blockade boosts cross-primed site I-specific T_{CD8} response

Tumor cells that supply cognate peptide:MHC I complexes (signal 1) along with a requisite costimulatory signal (signal 2) can directly activate naïve T_{CD8}. However, T_{CD8} responses to many tumors, especially those of non-hematopoietic origin, which do not express adequate costimulatory molecules (*e.g.*, CD80 and CD86) rely on cross-priming (51). In this pathway, professional APCs (pAPCs), such as DCs, acquire exogenous materials from tumor cells and process their proteins to form peptides, which are then complexed with MHC I and presented alongside costimulatory molecules to naïve T_{CD8}. We previously documented the *in vivo* significance of cross-priming for antitumor and antiviral immunity (43). Cross-priming also operates in the context of therapeutic vaccination to provoke anticancer T_{CD8} activation (52).

C57SV cells used in our immunization protocol should not directly prime naïve T_{CD8}. This is because: i) they are fibrosarcoma cells, not pAPCs; ii) they express neither costimulatory molecules such as CD40, CD80, CD86 and CD137L (Supplemental Fig. 2) nor MHC class II molecules (Supplemental Fig. 2) that would, at least in theory, enable them to recruit CD4$^+$ helper T cells; iii) they are transformed with subgenomic fragments of SV40 (43); ergo, they do not release SV40 virions that could otherwise infect host pAPCs to trigger direct priming. Nevertheless, to more definitively evaluate the beneficial effect of PD-1 blockade on cross-primed anticancer T_{CD8}, we administered anti-PD-1 to separate cohorts of B6 mice that were immunized with two other cell lines. TAP1$^{-/-}$ wt T Ag cells are syngeneic renal cells that cannot form peptide:MHC I complexes due to TAP mutation (45). KD2SV kidney epithelial cells are allogeneic (H-2^d) to B6 mice (H-2^b) and should not directly activate host T_{CD8} according to the rule of MHC restriction (53). Inoculation of B6 mice with either TAP1$^{-/-}$ wt T Ag or KD2SV cells resulted in detectable responses to sites I, II/III and IV, of which only the site I-specific response was boosted by anti-PD-1 (Fig. 5A–

B). Consequently, IFN-γ production upon *ex vivo* exposure to C57SV cells, which were used as a rough indicator of the overall T Ag-specific response, was also elevated. In the case of immunization with KD2SV cells, the effect of anti-PD-1 was so impressive that sites I-and IV-specific T_{CD8} became equidominant (Fig. 5B). This effect could also be recapitulated by using B6/K-TagI cells, which only express site I (46), in lieu of the corresponding peptide for *ex vivo* restimulation of splenocytes (Fig. 5B). Therefore, PD-1 blockade expands the site I-specific T_{CD8} clonal size, which is commensurate with a more rigorous response to site I displayed by either APCs or tumor cells.

It is noteworthy that *in vivo* priming of B6 mice with KD2SV cells also generates T_{CD8} alloreactivity to the mismatched MHC, which is independent of T Ag recognition. The allospecific response in this model can be detected after brief *ex vivo* stimulation of splenocytes with either H-2^{d+}T Ag^{+} cells (*e.g.*, KD2SV) or H-2^{d+}T Ag^{-} cells (*e.g.*, P815) (39, 40). In the experiment depicted in Fig. 5B, this response was also augmented upon treatment with anti-PD-1. To be precise, the mean frequencies (± SEM) of alloreactive IFN-γ^{+} T_{CD8} recognizing KD2SV cells were 8.19 ± 0.62 % in anti-PD-1-treated mice and 3.86 ± 0.82% in isotype-treated controls (p=0.005, n=4). Following a similar trend, alloreactive T_{CD8} responding to P815 cells *ex vivo* comprised 3.23 ± 0.26 % and 2.11 ± 0.46% of total splenic T_{CD8} in anti-PD-1- and isotype control-treated animals, respectively (p=0.043, n=4). It needs to be re-emphasized that as demonstrated in Fig. 5B and consistent with our previous studies (38–40, 43), T_{CD8} alloreactivity in this model does not alter the hierarchical pattern of syngeneic T_{CD8} responses to T Ag-derived epitopes, which we measure as an indication of cross-priming.

Taken together, the above findings imply that PD-1 blockade offers a previously unappreciated benefit through boosting subdominant T_{CD8} responses against many tumor cell types that are unable to activate naïve T cells on their own.

Anti-PD-1 increases the efficacy of SDD-targeting T_{CD8} vaccines only in the presence of co-existing IDD-specific T_{CD8} responses

In the next series of experiments, we sought to determine whether anti-PD-1 could also augment the response to site I in the context of therapeutic vaccination for cancer. B6 mice were immunized either with site I peptide-pulsed DCs (Fig. 6A) or with a recombinant vaccinia virus expressing the site I epitope as a cytosolic minigene (rVV-I mingene) (Fig. 6B), and treated with anti-PD-1 or isotype control. To our initial surprise, anti-PD-1 failed to increase the intensity of site I-specific T_{CD8} response and their absolute numbers in both models as evidenced by comparable *ex vivo* reactivity of splenocytes from anti-PD-1- and isotype-treated animals to site I peptide (Fig. 6A–B and data not shown), B6/K-TagI cells or C57SV cells (Fig. 6B and data not shown). Curiously however, when we used rVV-FL T Ag as a vaccine, anti-PD-1 increased both the frequency and the absolute number of site I-specific, IFN-γ^{+} T_{CD8} in the spleen (Fig. 6C and data not shown). In contrast, T_{CD8} responses to other T Ag epitopes, including site IV, were not altered.

Blocking PD-1-PD-L1 interactions rescues site I-specific T_{CD8} by removing the dominating effect of site IV-reactive T_{CD8}

Data shown in Fig. 6 suggested that site IV-specific T_{CD8} may 'dominate' their site I-specific counterparts through a PD-1-dependent mechanism. Immunodomination is experimentally defined as augmented reactivity to SDDs when responses to IDDS are diminished. To demonstrate this phenomenon in a T Ag-based tumor system, we first inoculated mice with B6/K-TagI cells, which lack all T Ag epitopes but site I (46). This was confirmed by detection of a robust T_{CD8} response against site I but no other epitopes, which could not be further strengthened upon anti-PD-1 treatment (Fig. 7A). We theorized that anti-PD-1 relieves immunodomination imposed by site IV-specific T_{CD8}. To test this hypothesis, we injected mice with B6/TpLM237-9Ab cells that are devoid of site IV only (47). As anticipated, the invigorating effect of anti-PD-1 on sites I- and II/III-specific T_{CD8} was abolished in this model (Fig. 7B).

To provide further evidence in support of the above theory, we next primed anti-PD-1- and isotype control-treated mice with peptide-pulsed BMDCs. A cohort of mice received mixed DC populations that were separately pulsed with site I and site IV peptides, and a parallel cohort received DCs that had been co-pulsed with both sites I and IV. We found treatment with anti-PD-1 to increase the site I-specific response, as judged by both ICS for IFN-γ and tetramer staining, only when co-pulsed DCs were used (Fig. 8A–B). Therefore, in order for the boosting effect of anti-PD-1 to manifest itself, site I- and site IV-specific T_{CD8} clones had to be in close proximity through engaging the same APCs. This is consistent with the hypothesis that PD-1 blockade increases the size of the site I-reactive clone by negating or mitigating the dominating behavior of site IV-specific T_{CD8}.

Treatment with anti-PD-1 prevents site I-specific T_{CD8} death

The mechanisms underlying immunodomination are not completely understood but may involve retarded subdominant T cell proliferation or their increased susceptibility to death. To find out which of these two scenarios could be reversed by the blockade of PD-1, we stained sites I- and IV-specific T_{CD8} for intracellular Ki-67 and active caspases on day 9 post-priming. Treatment with anti-PD-1 modestly decreased, rather than increased, the frequencies of tetramer-reactive cells that expressed the proliferation marker Ki-67 (Fig. 9A). In addition, the MFI of Ki-67 was comparable in both treatment groups (Fig. 9A). However, site I-specific T_{CD8} contained substantially more active caspases then did site IV-specific cells (Fig. 9B). Importantly, PD-1 blockade lowered the level of active caspases in site I- but not in site IV-specific T_{CD8}. Therefore, interfering with PD-1 triggering relieves immunodomination by preventing the lysis of subdominant T_{CD8} as opposed to promoting their proliferative growth.

Discussion

In this work, using a well-established model of antitumor T_{CD8} ID, we have uncovered a new role for PD-1-PD-L1 cross-talk in regulation of anticancer immunity. We found that PD-1-PD-L1 interaction is involved in a mechanism of immunodomination that selectively inhibits subdominant T_{CD8} responses to SV40 T Ag. Therefore, interfering with this

checkpoint pathway boosts SDD-specific T_{CD8}, which in turn increases the epitope breadth of the overall T_{CD8} response to T Ag. This finding is important because SDDs are capable of conferring protective immunity in certain conditions (54, 55). They are 'less visible' to the immune system and may thus escape central or peripheral tolerance mechanisms in mice (56, 57) and humans (58).

The model we employed is clinically relevant for multiple reasons. First, T Ag mediates neoplastic transformation of a variety of mammalian cell types (59). Second, SV40 T Ag is homologous to the BK virus T Ag detected in human kidneys (60). Third, a causal relationship has been recently established between the human Merkel cell polyomavirus large T Ag and a rare but aggressive type of cancer called Merkel cell carcinoma (MCC) (61, 62). Of note, the presence of T Ag-specific T_{CD8} in MCC tumors is correlated with better prognosis (63), and vaccination against a 'cryptic' epitope of this Ag has shown promise in a pre-clinical study (64).

One needs to refrain from discounting the role of immunodominant T_{CD8} in cancer as their significance (or lack thereof) can be cancer type-specific even when dealing with the same tumor Ag. In addition, *ex vivo* expanded IDD-specific T_{CD8} can be helpful once included in immunotherapeutic protocols. Previous work on SV40 large T Ag supports the above notions. In SV11 mice, which develop autochthonous T Ag-driven choroid plexus papillomas inside brain ventricles (65), endogenous T_{CD8} against T Ag epitopes are deleted due to negative selection in the thymus. However, adoptive transfer of naïve B6 splenocytes into sublethally irradiated SV11 mice results in extended control of tumors, which is associated with *in vivo* priming of site IV-specific immunodominant T_{CD8} among transferred splenocytes (66, 67) and the ability of splenocytes to produce IFN-γ (66). These observations simulate promising clinical results achieved in certain cancers after adoptive transfer of *ex vivo*-expanded autologous T_{CD8}, particularly when it is preceded by lymphodepletion (68, 69). On the other hand, in the transgenic adenocarcinoma of the mouse prostate (TRAMP) model (70), in which T Ag is expressed under the control of rat probasin promoter when male mice hit puberty, the response to site IV fizzles out with progression of the cancer. However, the immunorecessive site V-specific T_{CD8} escape thymic detection and avoid peripheral tolerance (71), thus providing opportunities for therapeutic interventions targeting this epitope.

We have used several different adjuvant strategies in the past in an attempt to boost subdominant T_{CD8} responses to T Ag, albeit to little avail. For example, when we inhibited IDO (39) or used an immunostimulatory dose of the mTOR inhibitor rapamycin (40), we could only boost the dominant response to site IV. Therefore, it appears that SDD-specific T_{CD8} responses are refractory to many forms of treatment. As such, the findings of our current work are important since treatment with anti-PD-1, but not with several other checkpoint inhibitors (data not shown), could remarkably boost the responsiveness of subdominant T_{CD8}. Accordingly, we propose that the beneficial effect of anti-PD-1 or anti-PD-L1 Abs in certain cancers may be, at least partially, due to their ability to augment subdominant T cell responses. By the same token, this effect may be absent in cancers that do not respond favorably to PD-1 blockade (*e.g.*, prostate cancer). In fact, anti-PD-1 monotherapy in TRAMP mice does not make T Ag-specific T_{CD8} clones detectable

regardless of their hierarchical position (our unpublished data). It is possible though that a combination of anti-PD-1 and other immuno-, radio- or chemotherapeutic modalities may exhibit additive or synergistic benefits. When we combined nTreg cell depletion and anti-PD-1, we noticed a greater effect on sites I- and II/III-specific responses, but none on site IV (Supplemental Fig. 3A–B). The additive nature of this strategy suggests that PD-1 blockade and nTreg depletion work through different mechanisms. We were also pleasantly surprised by the sudden appearance of a modest but reproducible response to site V (Supplemental Fig. 3A–C). Another tempting possibility that merits consideration is to combine PD-1-targeted therapies with approaches or agents that strengthen IDD-specific T_{CD8}, such as IDO and mTOR inhibitors (39, 40) among many others, in appropriate settings, in order to boost SDD- and IDD-specific clones alike.

From a mechanistic standpoint, several findings suggest that blocking PD-1-PD-L1 interactions could selectively boost subdominant clones by reversing their immunodomination by site IV-specific T_{CD8}. First, the observed rise in site I-specific T_{CD8} was numerical in essence, and these cells did not express higher levels of IFN-γ or CD107a, on a per cell basis, in anti-PD-1-treated animals. Second, although the beneficial effect of anti-PD-1 could also be demonstrated on memory T_{CD8} (Supplemental Fig. 1), this was also seemingly numerical and not due to an early commitment to generate more memory T_{CD8} precursors, which are phenotyped as $CD127^{high}KLRG1^{low}$ cells (40) (Supplemental Fig. 4). Third, the enhancing effect of anti-PD-1 was noticeable relatively late in the course of our kinetic studies, not during the initial priming by APCs (Fig. 3B). Fourth, in DC- and rVV-based immunization settings, in which we targeted site I alone, anti-PD-1 failed to elevate the response (Fig. 6A–B). Therefore, to conclusively demonstrate the ‘anti-immunodomination’ effect of PD-1 blockade, we used two different tumor cell lines expressing T Ags that lacked site IV. These experiments confirmed that PD-1 engagement indeed enforces site IV-mediated immunodomination. This conclusion was finally supported by our finding, in DC transfer experiments, that the selective enhancement of the site-I-directed response was evident only when site I- and site IV-specific T_{CD8} were physically adjacent and engaging the same APCs (Fig. 8A–B). To shed more light on this phenomenon, we sought to rule in or rule out the possibilities that the numerical rise in site I-specific T_{CD8} was owed to their increased proliferation or survival, scenarios that are not mutually exclusive. We found the frequency of Ki-67^+ cells among sites I- and IV-specific T_{CD8} to be moderately decreased, rather than increased. By contrast, only site I-specific T_{CD8} contained high levels of activate caspases, which could be lowered in anti-PD-1-treated mice. Therefore, PD-1 blockade prevents ‘lysis-dependent’ immunodomiantion of site I-specific T cells, which is unlike other mechanisms of immunodomination reported to date (27, 28, 41).

We found that C57SV cells, the T Ag^+ fibrosarcoma line that was frequently used in this investigation, do not express PD-L1 (Supplemental Fig. 2). Therefore, they should not be able to kill naïve T_{CD8} even in the unlikely event they might form stable and sustained immunological synapses with these cells. Moreover, if cross-presenting DCs had somehow selectively killed site I-specific T_{CD8} through a PD-L-1/PD-1-dependent mechanism, anti-PD-1 treatment should have enhanced the response to site I when it was presented alone and in the absence of other T Ag epitopes. On the other hand, cognate T_{CD8} cannot remove APCs during the priming phase since they are not yet armed with a cytotoxic arsenal. By

comparison, effector T_{CD8} may “bite the hands that feed them” by eliminating APCs (72). Nevertheless, this possibility too seems remote. If PD-L1 and PD-1 were sufficiently expressed by T_{CD8} and APCs, respectively, the effect of anti-PD-1 would likely have an indiscriminate effect on T_{CD8}. Since anti-PD-1 treatment selectively diminishes the intracellular caspase content of site I-specific T_{CD8} (Fig. 8B), we believe that blocking PD-1 prevents the fratricidal death of these cells.

It is currently unclear why subdominant site I-specific T_{CD8} express a higher level of PD-1 to begin with. Future investigations will address whether site I-specific T cells have a lower activation threshold resulting in swift, robust PD-1 expression and/or a propensity to retain PD-1 on their surface for a longer period of time. It is plausible to assume a link between the kinetics and stability of peptide:MHC complex formation for various IDDs and SDDs in the T Ag recognition model and the strength/sustenance of TCR triggering, which could in turn control the intensity of PD-1 expression. In addition, the balance/imbalance between a myriad of costimulatory and co-inhibitory signals should influence PD-1 expression and functions. This possibility is not far-fetched in light of findings in other models that CD40 ligation inhibits PD-1 induction (73) and that the efficacy of PD-1-based checkpoint inhibitor therapy is CD28-dependent (23).

To summarize our findings, our work reveals that ID hierarchies of antitumor T_{CD8} can be governed by PD-1-PD-L1 interactions. Blocking PD-1 broadens antitumor T_{CD8} responses, thus providing the host with more target choices, some of which may not evade immune detection or paralyze T cells. This represents a previously unrecognized effect of PD-1-targeted therapies. Interfering with PD-1 engagement blocks lysis-dependent immunodomination of subdominant T_{CD8}. By lifting this pressure, PD-1-targeted therapies reinvigorate subdominant T_{CD8} responses that can potentially contribute to antitumor immunity. These findings should be considered in PD-1-based immunotherapies and in rational vaccine design for cancer.

Supplementary Material

Refer to Web version on PubMed Central for supplementary material.

Acknowledgments

We thank members of the Haeryfar Laboratory for helpful discussions and Jeremy Haley for preparation of MHC tetramer reagents.

This research was supported by a Canadian Institutes of Health Research (CIHR) operating grant (MOP-130465) and by a Prostate Cancer Canada Movember Discovery Grant (D2014-16) (to S.M.M.H.), by a National Cancer Institute/National Institutes of Health grant (CA-025000) (to T.D.S.) and in part by the Intramural Research Program of the NIH, National Institute of Allergy and Infectious Diseases. C.E.M. is a recipient of an Alexander Graham Bell Canada Graduate Scholarship from Natural Sciences and Engineering Research Council of Canada, and C.R.S. is a CIHR postdoctoral fellowship recipient.

References

1. Gallimore A, Glithero A, Godkin A, Tissot AC, Pluckthun A, Elliott T, Hengartner H, Zinkernagel R. Induction and exhaustion of lymphocytic choriomeningitis virus-specific cytotoxic T

lymphocytes visualized using soluble tetrameric major histocompatibility complex class I-peptide complexes. J Exp Med. 1998; 187:1383–1393. [PubMed: 9565631]

2. Zajac AJ, Blattman JN, Murali-Krishna K, Sourdive DJ, Suresh M, Altman JD, Ahmed R. Viral immune evasion due to persistence of activated T cells without effector function. J Exp Med. 1998; 188:2205–2213. [PubMed: 9858507]
3. Sharma P, Allison JP. The future of immune checkpoint therapy. Science. 2015; 348:56–61. [PubMed: 25838373]
4. Wherry EJ, Kurachi M. Molecular and cellular insights into T cell exhaustion. Nat Rev Immunol. 2015; 15:486–499. [PubMed: 26205583]
5. Hoffmann M, Pantazis N, Martin GE, Hickling S, Hurst J, Meyerowitz J, Willberg CB, Robinson N, Brown H, Fisher M, Kinloch S, Babiker A, Weber J, Nwokolo N, Fox J, Fidler S, Phillips R, Frater J. Spartac, and C. Investigators. Exhaustion of Activated CD8 T Cells Predicts Disease Progression in Primary HIV-1 Infection. PLoS Pathog. 2016; 12:e1005661. [PubMed: 27415828]
6. McKinney EF, Lee JC, Jayne DR, Lyons PA, Smith KG. T-cell exhaustion, co-stimulation and clinical outcome in autoimmunity and infection. Nature. 2015; 523:612–616. [PubMed: 26123020]
7. Daud AI, Loo K, Pauli ML, Sanchez-Rodriguez R, Sandoval PM, Taravati K, Tsai K, Nosrati A, Nardo L, Alvarado MD, Algazi AP, Pampaloni MH, Lobach IV, Hwang J, Pierce RH, Gratz IK, Krummel MF, Rosenblum MD. Tumor immune profiling predicts response to anti-PD-1 therapy in human melanoma. J Clin Invest. 2016; 126:3447–3452. [PubMed: 27525433]
8. Barber DL, Wherry EJ, Masopust D, Zhu B, Allison JP, Sharpe AH, Freeman GJ, Ahmed R. Restoring function in exhausted CD8 T cells during chronic viral infection. Nature. 2006; 439:682–687. [PubMed: 16382236]
9. Ishida Y, Agata Y, Shibahara K, Honjo T. Induced expression of PD-1, a novel member of the immunoglobulin gene superfamily, upon programmed cell death. EMBO J. 1992; 11:3887–3895. [PubMed: 1396582]
10. Keir ME, Butte MJ, Freeman GJ, Sharpe AH. PD-1 and its ligands in tolerance and immunity. Annu Rev Immunol. 2008; 26:677–704. [PubMed: 18173375]
11. Pauken KE, Sammons MA, Odorizzi PM, Manne S, Godec J, Khan O, Drake AM, Chen Z, Sen DR, Kurachi M, Barnitz RA, Bartman C, Bengsch B, Huang AC, Schenkel JM, Vahedi G, Haining WN, Berger SL, Wherry EJ. Epigenetic stability of exhausted T cells limits durability of reinvigoration by PD-1 blockade. Science. 2016; 354:1160–1165. [PubMed: 27789795]
12. Araki K, Youngblood B, Ahmed R. Programmed cell death 1-directed immunotherapy for enhancing T-cell function. Cold Spring Harb Symp Quant Biol. 2013; 78:239–247. [PubMed: 25028401]
13. Chemnitz JM, Parry RV, Nichols KE, June CH, Riley JL. SHP-1 and SHP-2 associate with immunoreceptor tyrosine-based switch motif of programmed death 1 upon primary human T cell stimulation, but only receptor ligation prevents T cell activation. J Immunol. 2004; 173:945–954. [PubMed: 15240681]
14. Dong H, Zhu G, Tamada K, Chen L. B7-H1, a third member of the B7 family, co-stimulates T-cell proliferation and interleukin-10 secretion. Nat Med. 1999; 5:1365–1369. [PubMed: 10581077]
15. Freeman GJ, Long AJ, Iwai Y, Bourque K, Chernova T, Nishimura H, Fitz LJ, Malenkovich N, Okazaki T, Byrne MC, Horton HF, Fouser L, Carter L, Ling V, Bowman MR, Carreno BM, Collins M, Wood CR, Honjo T. Engagement of the PD-1 immunoinhibitory receptor by a novel B7 family member leads to negative regulation of lymphocyte activation. J Exp Med. 2000; 192:1027–1034. [PubMed: 11015443]
16. Tseng SY, Otsuji M, Gorski K, Huang X, Slansky JE, Pai SI, Shalabi A, Shin T, Pardoll DM, Tsuchiya H. B7-DC, a new dendritic cell molecule with potent costimulatory properties for T cells. J Exp Med. 2001; 193:839–846. [PubMed: 11283156]
17. Latchman Y, Wood CR, Chernova T, Chaudhary D, Borde M, Chernova I, Iwai Y, Long AJ, Brown JA, Nunes R, Greenfield EA, Bourque K, Boussiotis VA, Carter LL, Carreno BM, Malenkovich N, Nishimura H, Okazaki T, Honjo T, Sharpe AH, Freeman GJ. PD-L2 is a second ligand for PD-1 and inhibits T cell activation. Nat Immunol. 2001; 2:261–268. [PubMed: 11224527]
18. Wang X, Teng F, Kong L, Yu J. PD-L1 expression in human cancers and its association with clinical outcomes. Onco Targets Ther. 2016; 9:5023–5039. [PubMed: 27574444]

19. Ohaegbulam KC, Assal A, Lazar-Molnar E, Yao Y, Zang X. Human cancer immunotherapy with antibodies to the PD-1 and PD-L1 pathway. Trends Mol Med. 2015; 21:24–33. [PubMed: 25440090]
20. Hamanishi J, Mandai M, Matsumura N, Abiko K, Baba T, Konishi I. PD-1/PD-L1 blockade in cancer treatment: perspectives and issues. Int J Clin Oncol. 2016; 21:462–473. [PubMed: 26899259]
21. Pauken KE, Wherry EJ. Overcoming T cell exhaustion in infection and cancer. Trends Immunol. 2015; 36:265–276. [PubMed: 25797516]
22. O'Donnell JS, Long GV, Scolyer RA, Teng MW, Smyth MJ. Resistance to PD1/PDL1 checkpoint inhibition. Cancer Treat Rev. 2017; 52:71–81. [PubMed: 27951441]
23. Kamphorst AO, Wieland A, Nasti T, Yang S, Zhang R, Barber DL, Konieczny BT, Daugherty CZ, Koenig L, Yu K, Sica GL, Sharpe AH, Freeman GJ, Blazar BR, Turka LA, Owonikoko TK, Pillai R, Ramalingam SS, Araki K, Ahmed R. Rescue of exhausted CD8 T cells by PD-1-targeted therapies is CD28-dependent. Science. 2017; 355:1423–1427. [PubMed: 28280249]
24. Gilchuk P, Hill TM, Wilson JT, Joyce S. Discovering protective CD8 T cell epitopes--no single immunologic property predicts it! Curr Opin Immunol. 2015; 34:43–51. [PubMed: 25660347]
25. Yewdell JW, Bennink JR. Immunodominance in major histocompatibility complex class I-restricted T lymphocyte responses. Annu Rev Immunol. 1999; 17:51–88. [PubMed: 10358753]
26. Tscharke DC, Karupiah G, Zhou J, Palmore T, Irvine KR, Haeryfar SM, Williams S, Sidney J, Sette A, Bennink JR, Yewdell JW. Identification of poxvirus CD8+ T cell determinants to enable rational design and characterization of smallpox vaccines. J Exp Med. 2005; 201:95–104. [PubMed: 15623576]
27. Lin LC, Flesch IE, Tscharke DC. Immunodomination during peripheral vaccinia virus infection. PLoS Pathog. 2013; 9:e1003329. [PubMed: 23633956]
28. Chen W, Pang K, Masterman KA, Kennedy G, Basta S, Dimopoulos N, Hornung F, Smyth M, Bennink JR, Yewdell JW. Reversal in the immunodominance hierarchy in secondary CD8+ T cell responses to influenza A virus: roles for cross-presentation and lysis-independent immunodomination. J Immunol. 2004; 173:5021–5027. [PubMed: 15470045]
29. Crowe SR, Turner SJ, Miller SC, Roberts AD, Rappolo RA, Doherty PC, Ely KH, Woodland DL. Differential antigen presentation regulates the changing patterns of CD8+ T cell immunodominance in primary and secondary influenza virus infections. J Exp Med. 2003; 198:399–410. [PubMed: 12885871]
30. Probst HC, Tschannen K, Gallimore A, Martinic M, Basler M, Dumrese T, Jones E, van den Broek MF. Immunodominance of an antiviral cytotoxic T cell response is shaped by the kinetics of viral protein expression. J Immunol. 2003; 171:5415–5422. [PubMed: 14607945]
31. Gileadi U, Moins-Teisserenc HT, Correa I, Booth BL Jr, Dunbar PR, Sewell AK, Trowsdale J, Phillips RE, Cerundolo V. Generation of an immunodominant CTL epitope is affected by proteasome subunit composition and stability of the antigenic protein. J Immunol. 1999; 163:6045–6052. [PubMed: 10570292]
32. Zanker D, Waithman J, Yewdell JW, Chen W. Mixed proteasomes function to increase viral peptide diversity and broaden antiviral CD8+ T cell responses. J Immunol. 2013; 191:52–59. [PubMed: 23709680]
33. Deng Y, Yewdell JW, Eisenlohr LC, Bennink JR. MHC affinity, peptide liberation, T cell repertoire, and immunodominance all contribute to the paucity of MHC class I-restricted peptides recognized by antiviral CTL. J Immunol. 1997; 158:1507–1515. [PubMed: 9029084]
34. Chen W, Khilko S, Fecondo J, Margulies DH, McCluskey J. Determinant selection of major histocompatibility complex class I-restricted antigenic peptides is explained by class I-peptide affinity and is strongly influenced by nondominant anchor residues. J Exp Med. 1994; 180:1471–1483. [PubMed: 7523572]
35. Kotturi MF, Scott I, Wolfe T, Peters B, Sidney J, Cheroutre H, von Herrath MG, Buchmeier MJ, Grey H, Sette A. Naive precursor frequencies and MHC binding rather than the degree of epitope diversity shape CD8+ T cell immunodominance. J Immunol. 2008; 181:2124–2133. [PubMed: 18641351]

36. Leon-Ponte M, Kasprzyski T, Mannik LA, Haeryfar SM. Altered immunodominance hierarchies of influenza A virus-specific H-2(b)-restricted CD8+ T cells in the absence of terminal deoxynucleotidyl transferase. Immunol Invest. 2008; 37:714–725. [PubMed: 18821218]
37. Haeryfar SM, Hickman HD, Irvine KR, Tscharke DC, Bennink JR, Yewdell JW. Terminal deoxynucleotidyl transferase establishes and broadens antiviral CD8+ T cell immunodominance hierarchies. J Immunol. 2008; 181:649–659. [PubMed: 18566432]
38. Haeryfar SM, DiPaolo RJ, Tscharke DC, Bennink JR, Yewdell JW. Regulatory T cells suppress CD8+ T cell responses induced by direct priming and cross-priming and moderate immunodominance disparities. J Immunol. 2005; 174:3344–3351. [PubMed: 15749866]
39. Rytelewski M, Meilleur CE, Yekta MA, Szabo PA, Garg N, Schell TD, Jevnikar AM, Sharif S, Singh B, Haeryfar SM. Suppression of immunodominant antitumor and antiviral CD8+ T cell responses by indoleamine 2,3-dioxygenase. PLoS One. 2014; 9:e90439. [PubMed: 24587363]
40. Maleki Vareki S, Harding MJ, Waithman J, Zanker D, Shivji AN, Rytelewski M, Mazzuca DM, Yekta MA, Chen W, Schell TD, Haeryfar SM. Differential regulation of simultaneous antitumor and alloreactive CD8(+) T-cell responses in the same host by rapamycin. Am J Transplant. 2012; 12:233–239. [PubMed: 22026814]
41. Kedl RM, Rees WA, Hildeman DA, Schaefer B, Mitchell T, Kappler J, Marrack P. T cells compete for access to antigen-bearing antigen-presenting cells. J Exp Med. 2000; 192:1105–1113. [PubMed: 11034600]
42. Trinchieri G, Aden DP, Knowles BB. Cell-mediated cytotoxicity to SV40-specific tumour-associated antigens. Nature. 1976; 261:312–314. [PubMed: 179019]
43. Chen W, Masterman KA, Basta S, Haeryfar SM, Dimopoulos N, Knowles B, Bennink JR, Yewdell JW. Cross-priming of CD8+ T cells by viral and tumor antigens is a robust phenomenon. Eur J Immunol. 2004; 34:194–199. [PubMed: 14971045]
44. Knowles BB, Koncar M, Pfizenmaier K, Solter D, Aden DP, Trinchieri G. Genetic control of the cytotoxic T cell response to SV40 tumor-associated specific antigen. J Immunol. 1979; 122:1798–1806. [PubMed: 87443]
45. Otahal P, Hutchinson SC, Mylin LM, Tevethia MJ, Tevethia SS, Schell TD. Inefficient cross-presentation limits the CD8+ T cell response to a subdominant tumor antigen epitope. J Immunol. 2005; 175:700–712. [PubMed: 16002665]
46. Staveley-O'Carroll K, Schell TD, Jimenez M, Mylin LM, Tevethia MJ, Schoenberger SP, Tevethia SS. In vivo ligation of CD40 enhances priming against the endogenous tumor antigen and promotes CD8+ T cell effector function in SV40 T antigen transgenic mice. J Immunol. 2003; 171:697–707. [PubMed: 12847236]
47. Mylin LM, Deckhut AM, Bonneau RH, Kierstead TD, Tevethia MJ, Simmons DT, Tevethi SS. Cytotoxic T lymphocyte escape variants, induced mutations, and synthetic peptides define a dominant H-2Kb-restricted determinant in simian virus 40 tumor antigen. Virology. 1995; 208:159–172. [PubMed: 11831696]
48. Mylin LM, Schell TD, Roberts D, Epler M, Boesteanu A, Collins EJ, Frelinger JA, Joyce S, Tevethia SS. Quantitation of CD8(+) T-lymphocyte responses to multiple epitopes from simian virus 40 (SV40) large T antigen in C57BL/6 mice immunized with SV40, SV40 T-antigen-transformed cells, or vaccinia virus recombinants expressing full-length T antigen or epitope minigenes. J Virol. 2000; 74:6922–6934. [PubMed: 10888631]
49. Grabarek J, Amstad P, Darzynkiewicz Z. Use of fluorescently labeled caspase inhibitors as affinity labels to detect activated caspases. Hum Cell. 2002; 15:1–12. [PubMed: 12126059]
50. Fu TM, Mylin LM, Schell TD, Bacik I, Russ G, Yewdell JW, Bennink JR, Tevethia SS. An endoplasmic reticulum-targeting signal sequence enhances the immunogenicity of an immunorecessive simian virus 40 large T antigen cytotoxic T-lymphocyte epitope. J Virol. 1998; 72:1469–1481. [PubMed: 9445050]
51. Bevan MJ. Cross-priming for a secondary cytotoxic response to minor H antigens with H-2 congenic cells which do not cross-react in the cytotoxic assay. J Exp Med. 1976; 143:1283–1288. [PubMed: 1083422]

52. Melief CJ. Mini-review: Regulation of cytotoxic T lymphocyte responses by dendritic cells: peaceful coexistence of cross-priming and direct priming? Eur J Immunol. 2003; 33:2645–2654. [PubMed: 14515248]

53. Zinkernagel RM, Doherty PC. Restriction of in vitro T cell-mediated cytotoxicity in lymphocytic choriomeningitis within a syngeneic or semiallogeneic system. Nature. 1974; 248:701–702. [PubMed: 4133807]

54. Ryan CM, Schell TD. Accumulation of CD8+ T cells in advanced-stage tumors and delay of disease progression following secondary immunization against an immunorecessive epitope. J Immunol. 2006; 177:255–267. [PubMed: 16785521]

55. Feltkamp MC, Vreugdenhil GR, Vierboom MP, Ras E, van der Burg SH, ter Schegget J, Melief CJ, Kast WM. Cytotoxic T lymphocytes raised against a subdominant epitope offered as a synthetic peptide eradicate human papillomavirus type 16-induced tumors. Eur J Immunol. 1995; 25:2638–2642. [PubMed: 7589138]

56. Schell TD. In vivo expansion of the residual tumor antigen-specific CD8+ T lymphocytes that survive negative selection in simian virus 40 T-antigen-transgenic mice. J Virol. 2004; 78:1751–1762. [PubMed: 14747540]

57. Uram JN, Black CM, Flynn E, Huang L, Armstrong TD, Jaffee EM. Nondominant CD8 T cells are active players in the vaccine-induced antitumor immune response. J Immunol. 2011; 186:3847–3857. [PubMed: 21346233]

58. Friedman RS, Spies AG, Kalos M. Identification of naturally processed CD8 T cell epitopes from prostein, a prostate tissue-specific vaccine candidate. Eur J Immunol. 2004; 34:1091–1101. [PubMed: 15048720]

59. Livingston DM, Bradley MK. The simian virus 40 large T antigen. A lot packed into a little. Mol Biol Med. 1987; 4:63–80. [PubMed: 3041175]

60. Seif I, Khoury G, Dhar R. The genome of human papovavirus BKV. Cell. 1979; 18:963–977. [PubMed: 229976]

61. Kassem A, Schopflin A, Diaz C, Weyers W, Stickeler E, Werner M, Zur Hausen A. Frequent detection of Merkel cell polyomavirus in human Merkel cell carcinomas and identification of a unique deletion in the VP1 gene. Cancer Res. 2008; 68:5009–5013. [PubMed: 18593898]

62. Houben R, Shuda M, Weinkam R, Schrama D, Feng H, Chang Y, Moore PS, Becker JC. Merkel cell polyomavirus-infected Merkel cell carcinoma cells require expression of viral T antigens. J Virol. 2010; 84:7064–7072. [PubMed: 20444890]

63. Sihto H, Bohling T, Kavola H, Koljonen V, Salmi M, Jalkanen S, Joensuu H. Tumor infiltrating immune cells and outcome of Merkel cell carcinoma: a population-based study. Clin Cancer Res. 2012; 18:2872–2881. [PubMed: 22467679]

64. Gomez BP, Wang C, Viscidi RP, Peng S, He L, Wu TC, Hung CF. Strategy for eliciting antigen-specific CD8+ T cell-mediated immune response against a cryptic CTL epitope of merkel cell polyomavirus large T antigen. Cell Biosci. 2012; 2:36. [PubMed: 23095249]

65. Brinster RL, Chen HY, Messing A, van Dyke T, Levine AJ, Palmiter RD. Transgenic mice harboring SV40 T-antigen genes develop characteristic brain tumors. Cell. 1984; 37:367–379. [PubMed: 6327063]

66. Tatum AM, Mylin LM, Bender SJ, Fischer MA, Vigliotti BA, Tevethia MJ, Tevethia SS, Schell TD. CD8+ T cells targeting a single immunodominant epitope are sufficient for elimination of established SV40 T antigen-induced brain tumors. J Immunol. 2008; 181:4406–4417. [PubMed: 18768900]

67. Schell TD, Tevethia SS. Control of advanced choroid plexus tumors in SV40 T antigen transgenic mice following priming of donor CD8(+) T lymphocytes by the endogenous tumor antigen. J Immunol. 2001; 167:6947–6956. [PubMed: 11739514]

68. Dudley ME, Wunderlich JR, Yang JC, Sherry RM, Topalian SL, Restifo NP, Royal RE, Kammula U, White DE, Mavroukakis SA, Rogers LJ, Gracia GJ, Jones SA, Mangiameli DP, Pelletier MM, Gea-Banacloche J, Robinson MR, Berman DM, Filie AC, Abati A, Rosenberg SA. Adoptive cell transfer therapy following non-myeloablative but lymphodepleting chemotherapy for the treatment of patients with refractory metastatic melanoma. J Clin Oncol. 2005; 23:2346–2357. [PubMed: 15800326]

69. Dudley ME, Wunderlich JR, Robbins PF, Yang JC, Hwu P, Schwartzentruber DJ, Topalian SL, Sherry R, Restifo NP, Hubicki AM, Robinson MR, Raffeld M, Duray P, Seipp CA, Rogers-Freezer L, Morton KE, Mavroukakis SA, White DE, Rosenberg SA. Cancer regression and autoimmunity in patients after clonal repopulation with antitumor lymphocytes. Science. 2002; 298:850–854. [PubMed: 12242449]

70. Greenberg NM, DeMayo F, Finegold MJ, Medina D, Tilley WD, Aspinall JO, Cunha GR, Donjacour AA, Matusik RJ, Rosen JM. Prostate cancer in a transgenic mouse. Proc Natl Acad Sci U S A. 1995; 92:3439–3443. [PubMed: 7724580]

71. Grossmann ME, Davila E, Celis E. Avoiding Tolerance Against Prostatic Antigens With Subdominant Peptide Epitopes. J Immunother (1991). 2001; 24:237–241. [PubMed: 11395639]

72. Tscharke DC, Yewdell JW. T cells bite the hand that feeds them. Nat Med. 2003; 9:647–648. [PubMed: 12778158]

73. Isogawa M, Chung J, Murata Y, Kakimi K, Chisari FV. CD40 activation rescues antiviral CD8(+) T cells from PD-1-mediated exhaustion. PLoS Pathog. 2013; 9:e1003490. [PubMed: 23853599]

Abbreviations used in this article

B6	C57BL/6
BMDCs	bone marrow-derived dendritic cells
DC(s)	dendritic cell(s)
FLICA	fluorochrome-labeled inhibitors of caspases
ICS	intracellular cytokine staining
ID	immunodominance
IDD(s)	immunodominant determinant(s)
MCC	Merkel cell carcinoma
MFI	mean fluorescence intensity
mTOR	mammalian target of rapamycin
nT_{reg}	naturally occurring regulatory T cell(s)
pAPC(s)	professional APC(s)
PEC(s)	peritoneal exudate cell(s)
SDD(s)	subdominant determinant(s)
T Ag	SV40-encoded large tumor antigen
T_{CD8}	$CD8^+$ T cell(s)
TRAMP	transgenic adenocarcinoma of the mouse prostate
rVV	recombinant vaccinia virus
rVV-FL	T Ag, recombinant vaccinia virus expressing full-length large tumor antigen

rVV-I minigene	recombinant vaccinia virus expressing site I minigene
SHP	src homology 2-containing tyrosine phosphatase;

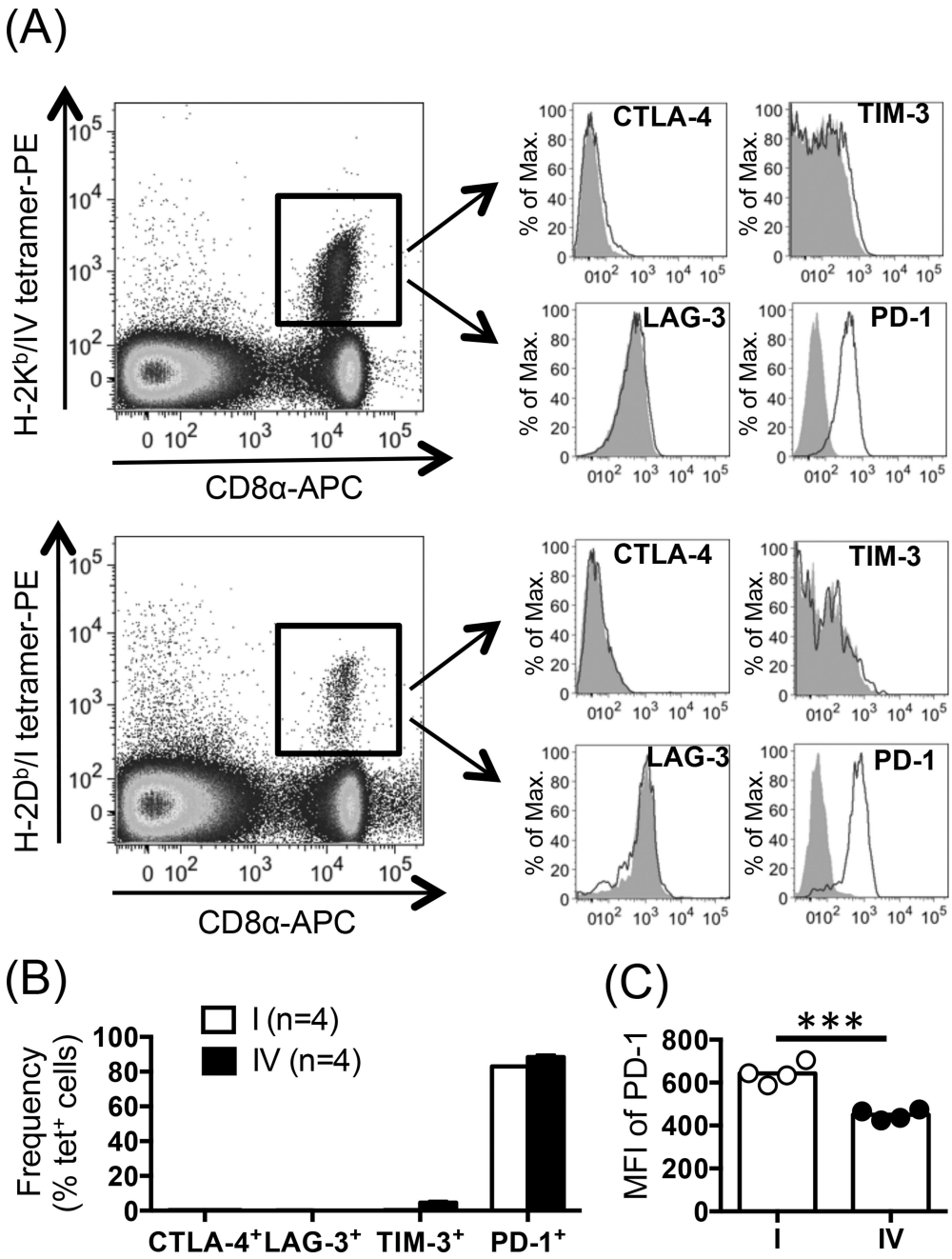

Fig. 1.

PD-1 is highly expressed by site I-specific T_{CD8}. (A) Nine days after inoculation of B6 mice (n=4) with T Ag^+ C57SV fibrosarcoma cells, site I- and site IV-specific T_{CD8} were identified in the spleens via co-staining with an anti-CD8α mAb and indicated MHC I tetramers. (B–C) Further analysis was conducted to determine the frequency of CTLA-4^+, LAG-3^+, TIM-3^+ or PD-1^+ cells among sites I- and IV-specific T_{CD8} (B) and to calculate the MFI of PD-1 expression for each population (C). Representative histograms are illustrated (*A*), and bar graphs depict the results obtained from 4 mice (B–C). Circles (C) indicate

biological replicates, and error bars (B–C) represent SEM. Statistical analysis was performed using unpaired Student's *t*-test (n=4; *** p<0.001) (C).

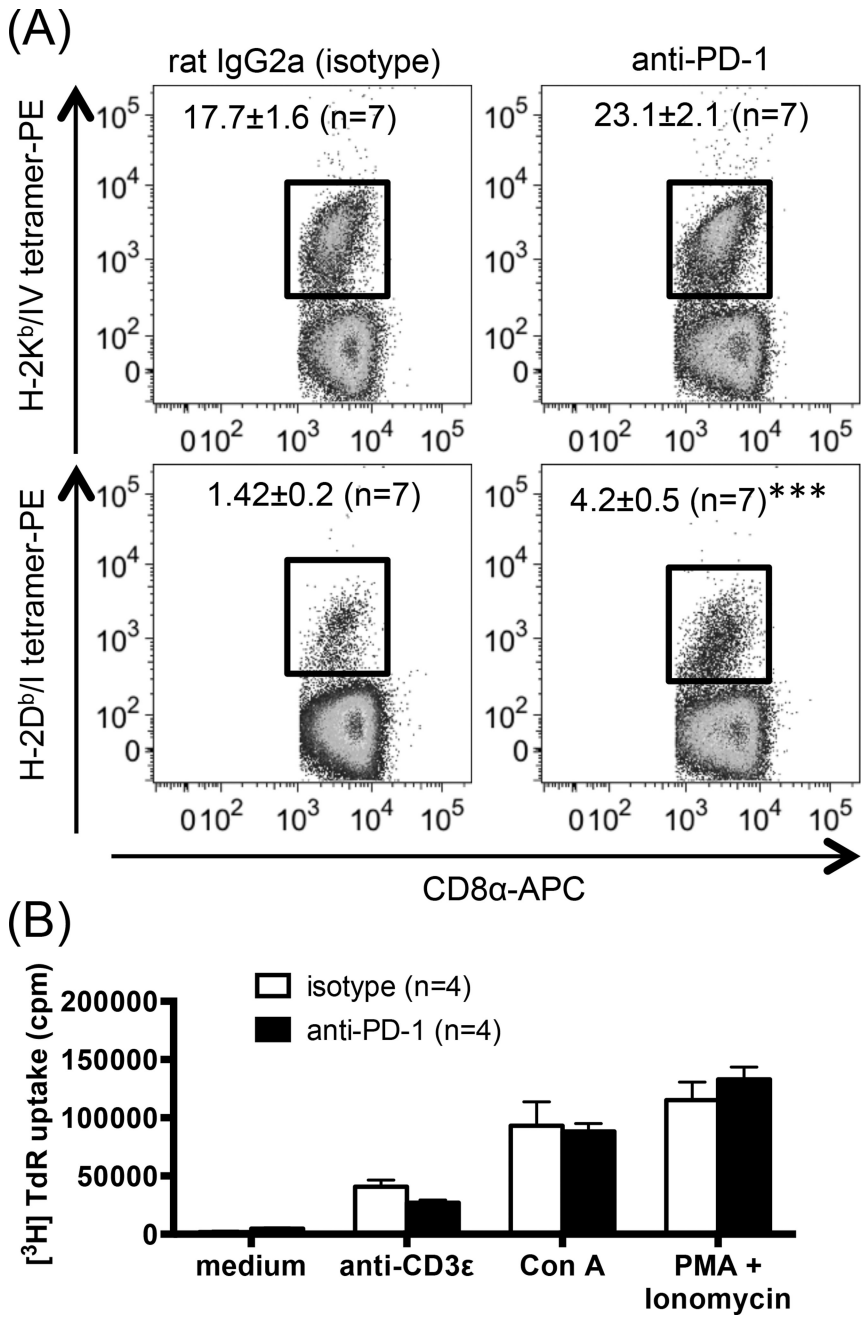

Fig. 2.

Treatment with anti-PD-1 increases the clonal size of splenic site I-specific T_{CD8}, but not global splenocyte responses to non-specific stimuli. (A) B6 mice were inoculated i.p. with C57SV cells and treated with 3 separate doses of an anti-PD-1 mAb or isotype control (n=4 per group). Nine days later, splenic sites I- and IV-specific T_{CD8} were detected by tetramer staining. Representative dot plots are depicted, and mean ± SEM values (n=7 per group) are indicated. Statistical comparisons between anti-PD-1- and isotype-treated mice (n=7 per group) were carried out by unpaired Student's *t*-test (*** $p<0.001$). (B) Bulk B6 splenocytes (n=4 mice per group) were stimulated for 72 h with indicated mitogens. Cells were exposed

to tritiated thymidine ([^{3}H]TdR) during the final 18 h of cultures, and [^{3}H]TdR incorporation was quantitated.

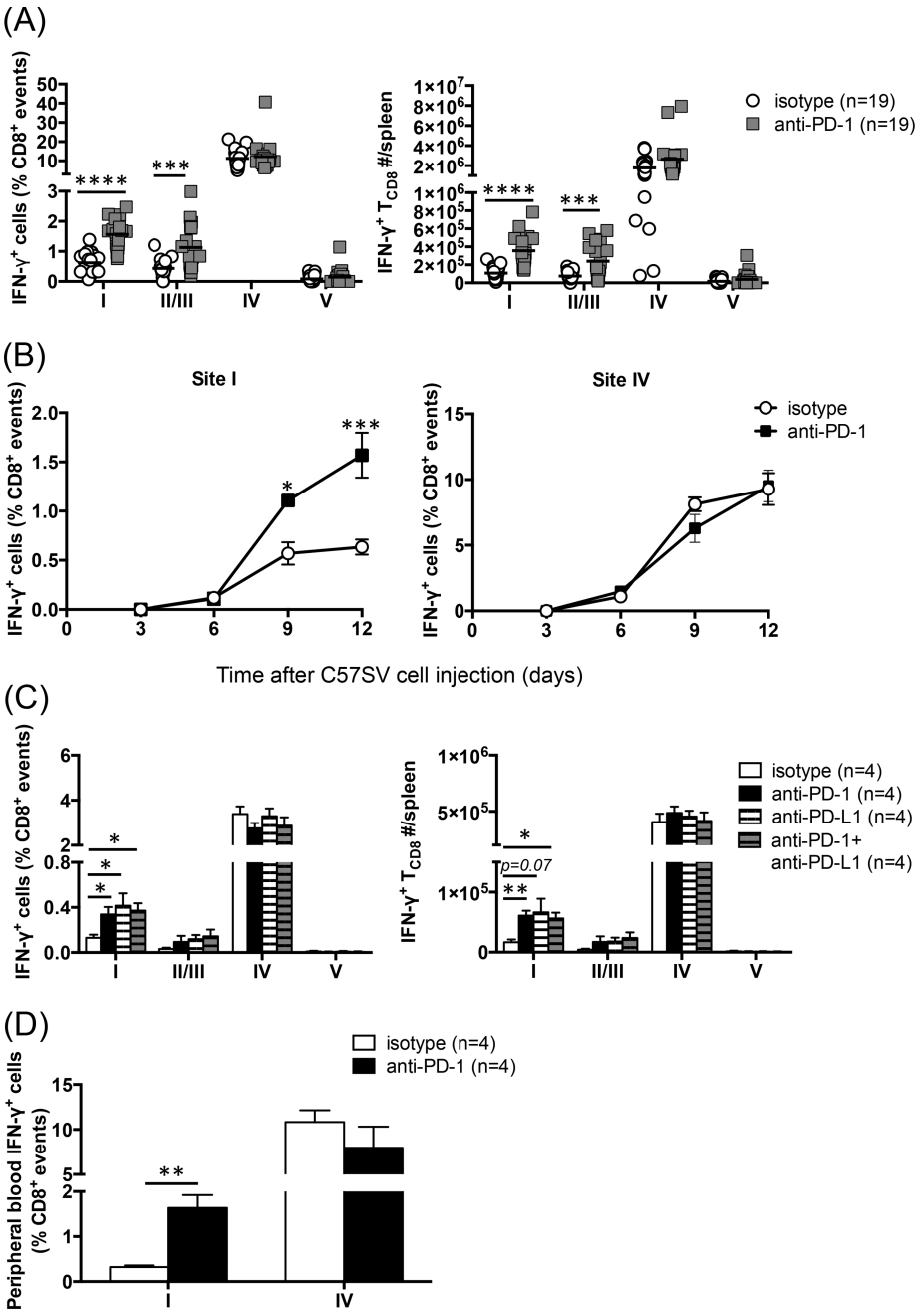

Fig. 3.

Blocking PD-1-PD-L1 interaction increases the frequencies and absolute numbers of IFN-γ-producing subdominant T_{CD8}. (A) Mice were primed with C57SV cells and treated with 3 separate doses of an anti-PD-1 mAb or isotype control (n=19 per group). Nine days later, the percentages of sites I- , II/III, IV- and V-specific T_{CD8} (A; left panel) and their absolute numbers (A; right panel) in each spleen were determined by ICS for IFN-γ. Each circle or square represents an individual mouse. *** and **** denote statistical differences with $p<0.001$ and $p<0.0001$, respectively, which were calculated by unpaired Student's *t*-test. (B) Separate cohorts of mice were injected with C57SV cells and treated with anti-PD-1 or

isotype control (n=4 per group). Sites I- and IV-specific T_{CD8} frequencies were determined at indicated time points by ICS. Statistical comparisons between anti-PD-1- and isotype-treated mice were performed by two-way ANOVA ($p<0.05$) with Holm-Sidak post-hoc analysis (* and *** denote $p<0.05$ and $p<0.001$, respectively). (C) C57SV-primed mice were treated with anti-PD-1, anti-PD-L1, or a combination of both mAbs, or isotype controls (n=4 per group). T_{CD8} responses to indicated epitopes were quantified by ICS for IFN-γ on day 9 post-priming. Student's *t*-test was employed for statistical analyses, and * denotes $p<0.05$. Error bars (A–C) represent SEM. (D) B6 mice were injected with C57SV cells and treated with 3 doses of anti-PD-1 or isotype control (n=4 per group). Nine days after tumor cell injection, the frequencies of sites I- and IV-specific IFN-g-producing T_{CD8} among PBMCs were determined by flow cytometry. ** denotes a statistical difference with $p<0.01$.

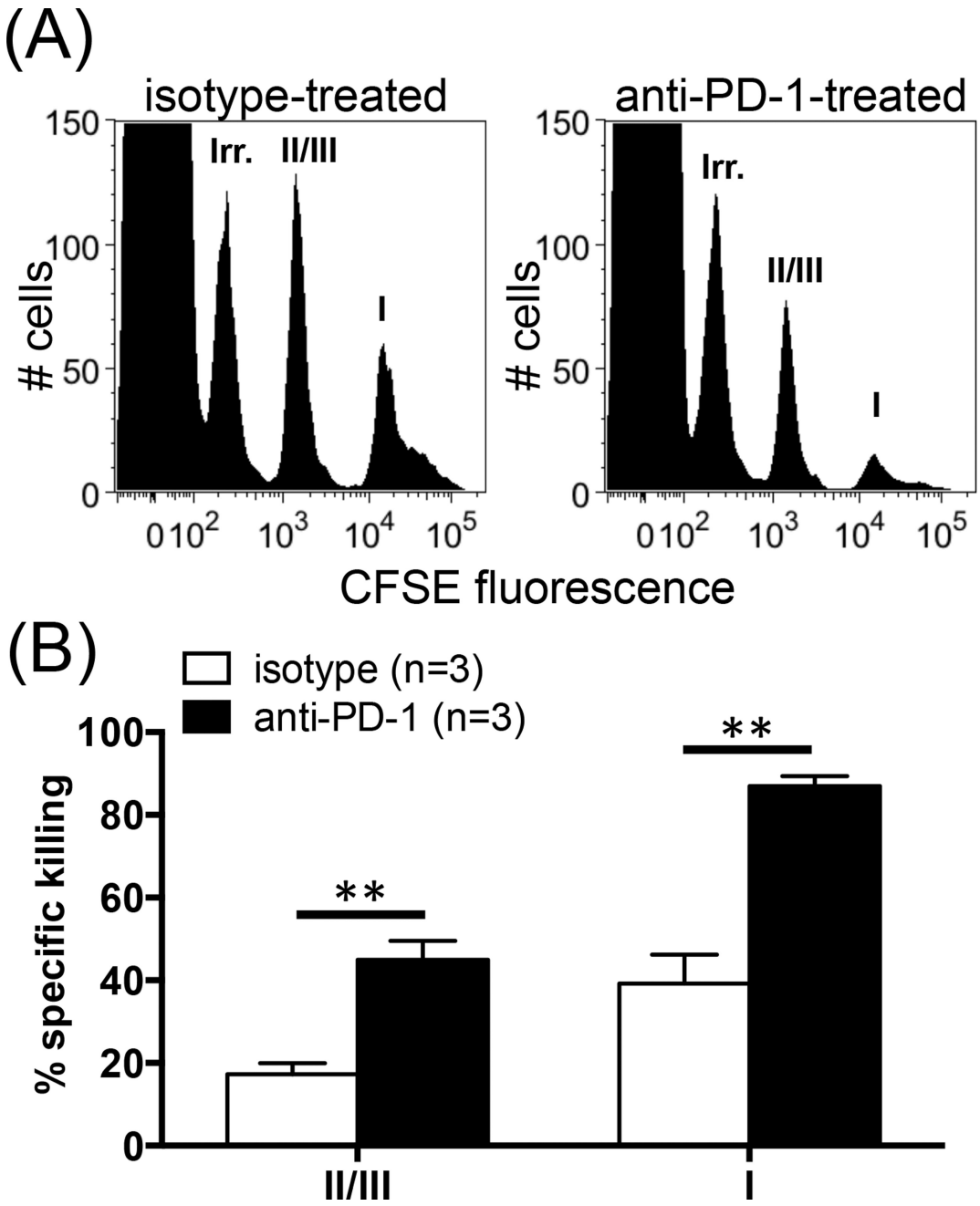

Fig. 4.

Anti-PD-1 treatment augments subdominant T_{CD8}-mediated cytotoxicity. Target cells were prepared by pulsing syngeneic naïve splenocytes with gB_{498} (irrelevant peptide), site II/III peptide or site I peptide, which were labeled with 0.025 μM, 0.25 μM and 2 μM CFSE, respectively. Target cells were mixed in equal numbers and injected into the tail vein of C57SV-primed mice that had received anti-PD-1 or isotype control (n=3 per group). Four h later, target cell populations were tracked by flow cytometry in each spleen (A), and their % specific lysis was calculated (B). ** denotes a statistical difference with $p<0.01$ by unpaired Student's *t*-test. Error bars (B) represent SEM.

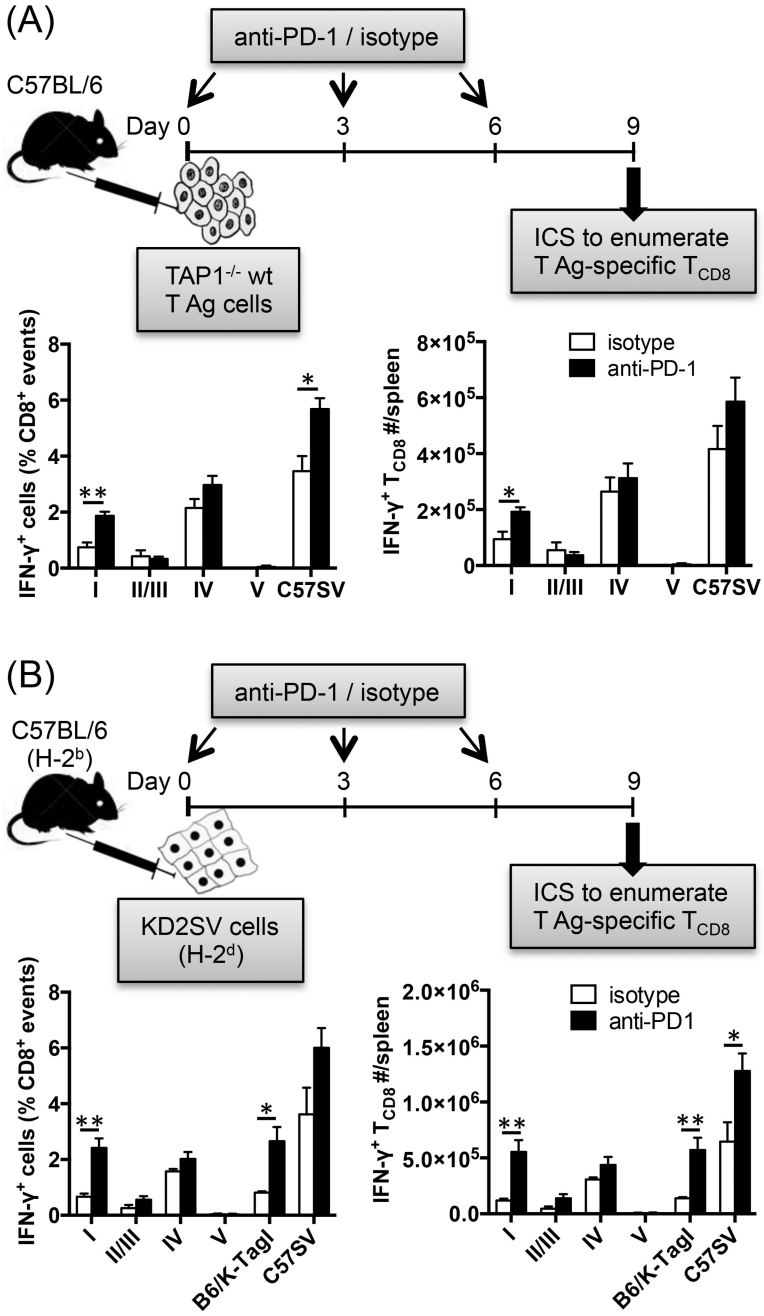

Fig. 5.

PD-1 blockade enhances the magnitude of cross-primed site I-specific T_{CD8} response. B6 mice were injected i.p. with $TAP1^{-/-}$ wt T Ag cells (A) or KD2SV cells (B) and treated with either anti-PD-1 or isotype control (n=4 per cohort). Nine days later, the frequencies (left panels) and absolute numbers (right panels) of splenic T Ag-specific T_{CD8} were determined by ICS for IFN-γ after brief *ex vivo* stimulation with indicated T Ag-derived peptides or T Ag^+ cell lines. * and ** denote $p<0.05$ and $p<0.01$, respectively, which were calculated by Student's *t*-test. Error bars (A–B) represent SEM.

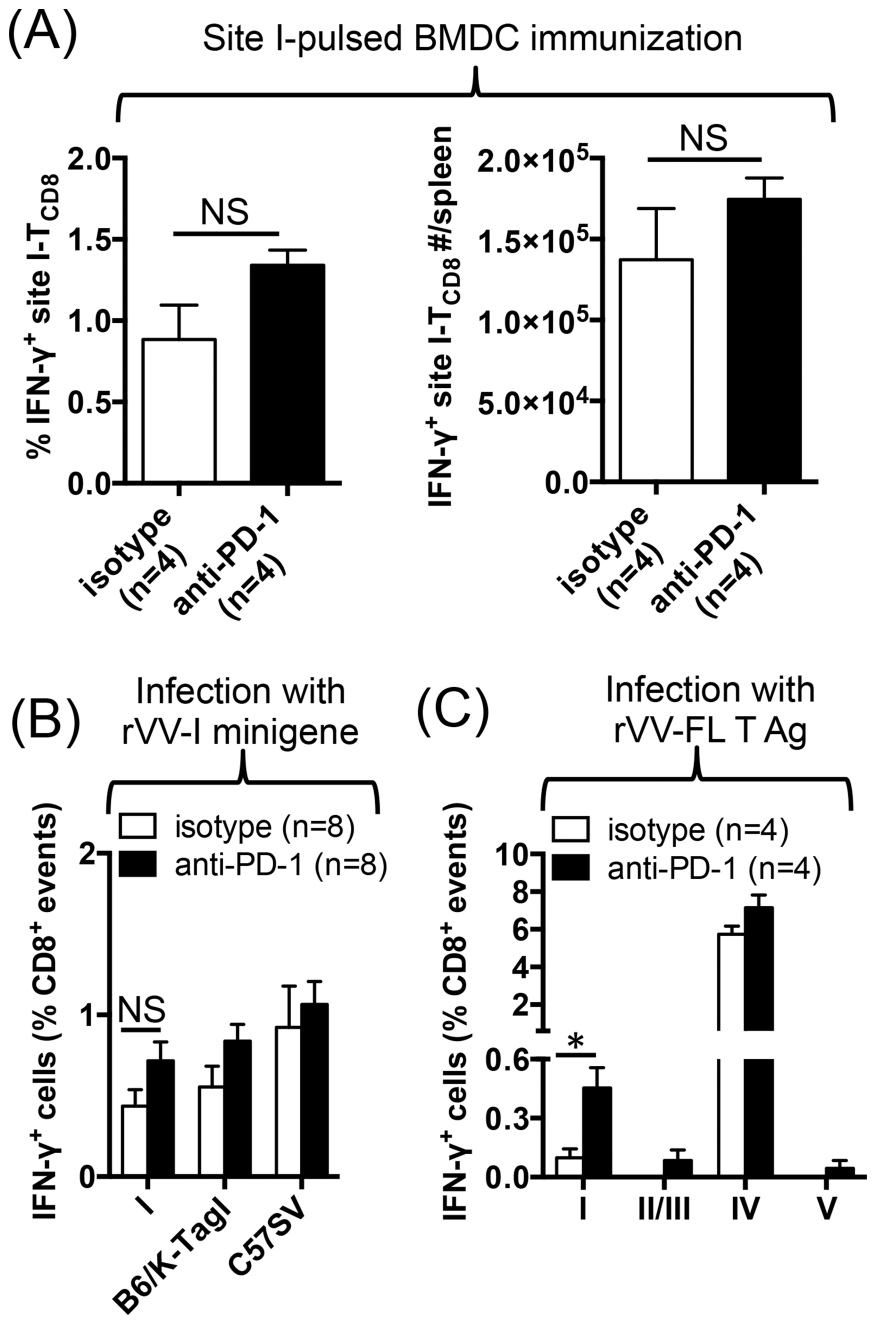

Fig. 6.

Anti-PD-1 boosts the efficacy of vaccination against site I only when a site IV-specific response is co-present. B6 mice were injected i.v. with site I peptide-pulsed BMDCs (A) or infected i.p. with either rVV-I minigene (B) or rVV-FL T Ag (C) before they received treatment with anti-PD-1 or isotype control (n=4–8 per cohort as indicated). Seven days later, T Ag-specific T_{CD8} responses were quantified by ICS after *ex vivo* stimulation of splenocytes with indicated T Ag-derived peptides or T Ag^+ cell lines. * denotes $p<0.05$ by Student's *t*-test (C). NS: non-significant (A–B). Error bars (A–C) represent SEM.

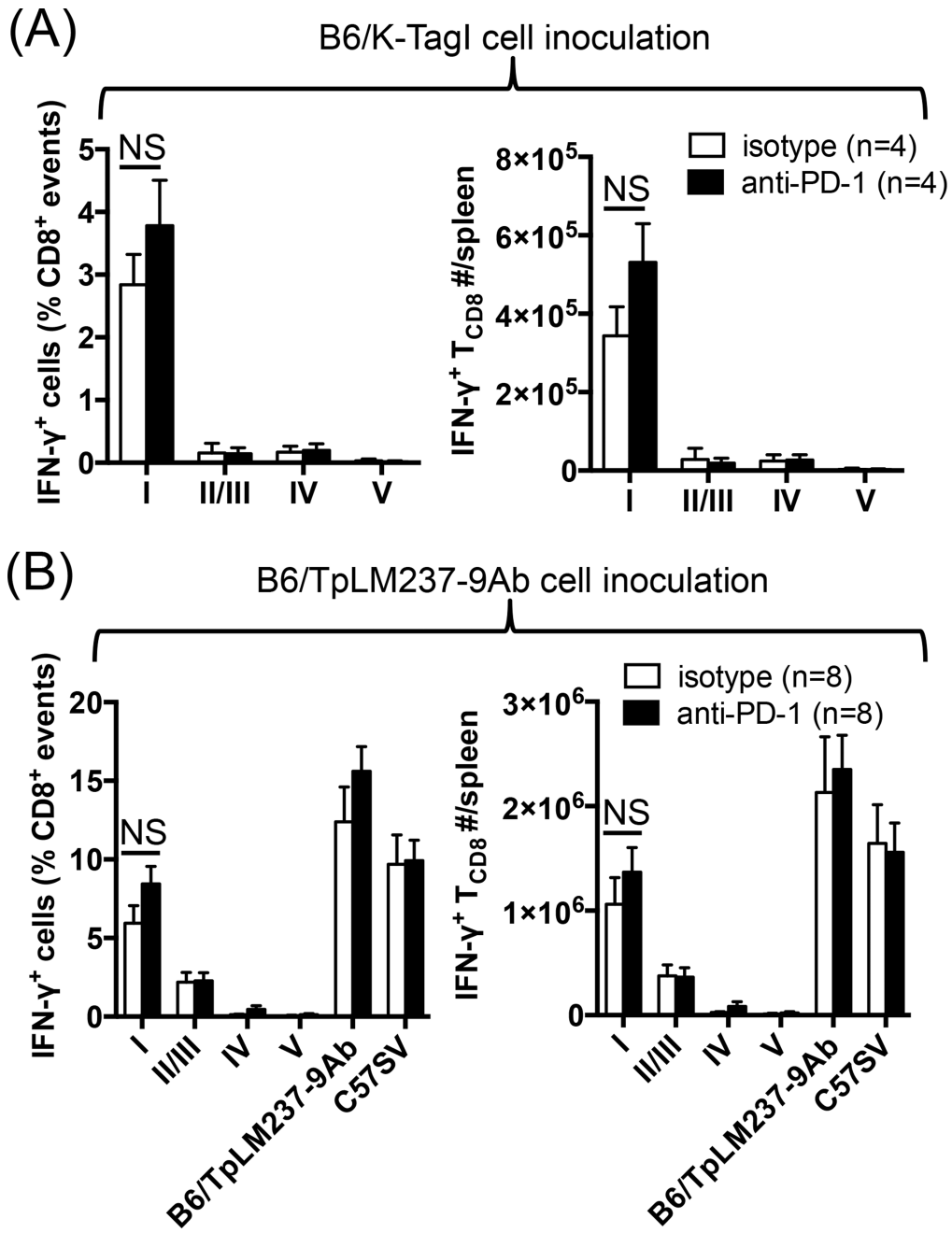

Fig. 7.

Anti-PD-1 fails to elevate the magnitude of site I-specific response following immunization with site IV-negative tumor cells. Mice were injected i.p. with B6/K-TagI cells (A) or B6/TpLM237-9Ab cells (B) and treated with either anti-PD-1 or isotype control (n=4 per cohort). Nine days later, the frequencies (left panels) and absolute numbers (right panels) of splenic T Ag-specific T_{CD8} were determined by ICS after *ex vivo* stimulation of splenocytes with indicated T Ag-derived peptides (A–B) or T Ag^+ cell lines (B). Error bars (A–B) represent SEM. NS: non-significant (A–B)

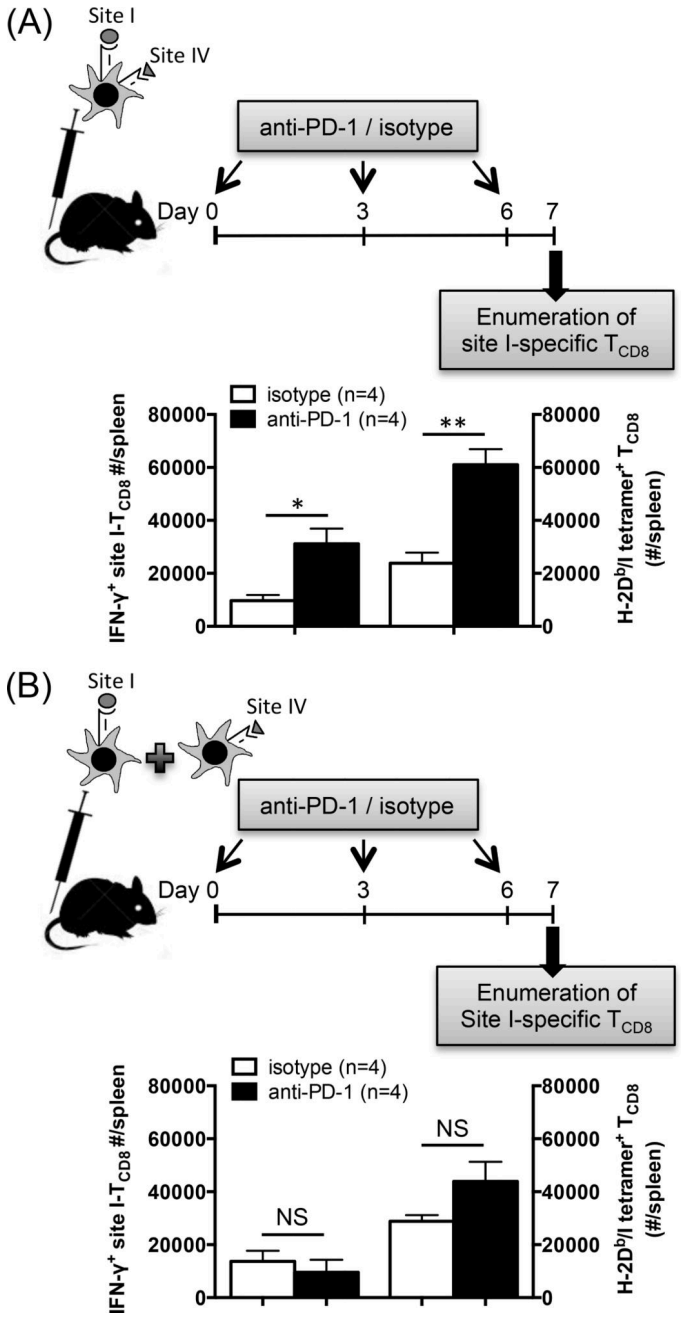

Fig. 8.

Anti-PD-1 invigorates the site I-specific T_{CD8} response following immunization with DCs simultaneously displaying sites I and IV. B6 mice were injected i.v. with BMDCs co-pulsed with synthetic peptides corresponding to sites I and IV (A) or with mixed BMDC populations separately pulsed with each peptide alone (B) before they were treated with anti-PD-1 or isotype control (n=4 per cohort). Seven days later, mice were sacrificed, and splenic site I-specific T_{CD8} were enumerated by ICS for IFN-γ and by tetramer staining in parallel. * and ** denote $p<0.05$ and $p<0.01$, respectively, by Student's *t*-test (A). Error bars represent SEM (A–B). NS: non-significant (B)

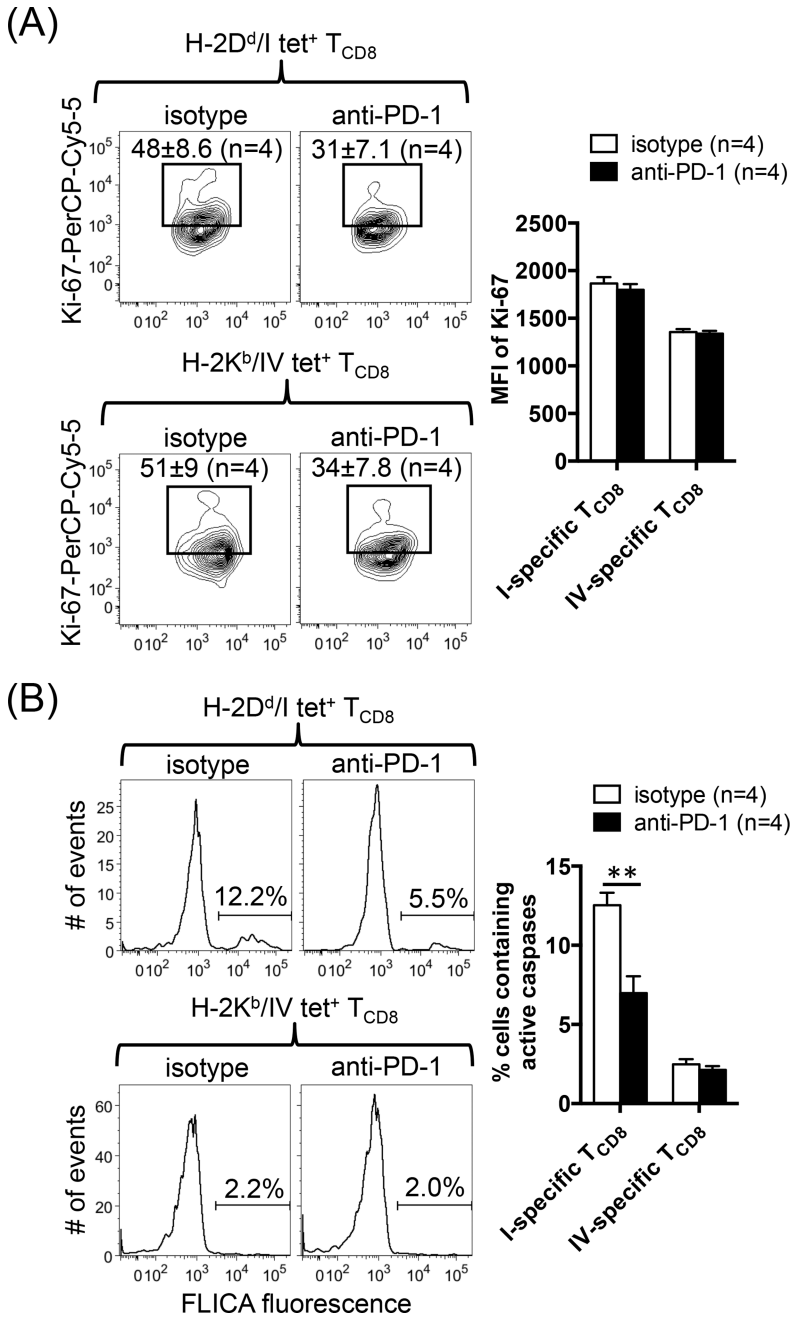

Fig. 9.

PD-1 blockade enhances site I-specific T_{CD8} survival but not their proliferative capacity. (A) Nine days after priming with C57SV cells, the frequencies of Ki-67$^+$ cells and the MFI of Ki-67 expression within splenic sites I- and IV-specific T_{CD8} populations were determined in anti-PD-1-treated and control mice. Representative contour plots and mean ± SEM values are shown for 4 mice per group. (B) FLICA fluorescence as an active indicator of intracellular caspase levels was also assessed by flow cytometry. Representative histograms

are illustrated, and bar graphs depict the results obtained from 4 mice per group (B). Error bars (A–B) represent SEM, and ** denotes $p<0.01$ by Student's *t*-test (B).

Table 1

Peptides used in this study

Protein Ag Source	Peptide Epitope	Designation	Sequence	Restricting MHC I
SV40 Large T Ag	$T\ Ag_{206–215}$	Site I	SAINNYAQKL	$H\text{-}2D^b$
SV40 Large T Ag	$T\ Ag_{223–231}$	Site II/III	CKGVNKEYL	$H\text{-}2D^b$
SV40 Large T Ag	$T\ Ag_{404–411}$	Site IV	VVYDFLKC	$H\text{-}2K^b$
SV40 Large T Ag	$T\ Ag_{489–497}$	Site V	QGINNLDNL	$H\text{-}2D^b$
HSV-1 Glycoprotein B	$gB_{498–505}$	gB_{498}	SSIEFARL	$H\text{-}2K^b$